JAERI-Research
97-082

SYSTEMATIC STUDY ON SPUTTERING YIELDS BY 14.9 MeV NEUTRONS

November 1997

Bangjiao YE※, Yoshimi KASUGAI and Yujiro IKEDA

日本原子力研究所
Japan Atomic Energy Research Institute

本レポートは，日本原子力研究所が不定期に公刊している研究報告書です。

入手の問合わせは，日本原子力研究所研究情報部研究情報課（〒319-11 茨城県那珂郡東海村）あて，お申し越しください。なお，このほかに財団法人原子力弘済会資料センター（〒319-11 茨城県那珂郡東海村日本原子力研究所内）で複写による実費頒布をおこなっております。

This report is issued irregularly.

Inquiries about availability of the reports should be addressed to Research Information Division, Department of Intellectual Resources, Japan Atomic Energy Research Institute, Tokai-mura, Naka-gun, Ibaraki-ken, 319-11, Japan.

編集兼発行　日本原子力研究所
印　　刷　いばらき印刷(株)

Systematic Study on Sputtering Yields by 14.9 MeV Neutrons

Bangjiao YE[※], Yoshimi KASUGAI and Yujiro IKEDA

Department of Reactor Engineering
Tokai Research Establishment
Japan Atomic Energy Research Institute
Tokai-mura, Naka-gun, Ibaraki-ken

(Received October 15, 1997)

Neutron sputtering yields have been measured for radioactive nuclide production reactions at a 14.9 MeV neutron energy. Materials investigated were F, Mg, Al, Sc, Ti, V, Cr, Fe, Co, Ni, Cu, Zr, Nb, Mo, Pd, Ag, Cd, In, Ta, Re, Pt, Au, Pb and SS316. The 14.9 MeV neutrons were produced by a D-T neutron generator at the Fusion Neutronics Source (FNS). The sputtered radioactive materials deposited on the collectors were investigated by the neutron activation analysis. In this work, all measurements were performed in air. Several different distances between the sample and the collector of the sputtered materials were chosen to be 0.2, 0.5, 1.0, 2.0, 3.0 and 5.0 mm to deduce the sputtering yield. The sputtering yields of fifty-seven reactions belonging to (n, 2n), (n, α), (n, p) and (n, np) have been measured. The systematics for reduced sputtering yield as a function of the atomic number (Z) have been derived for (n, 2n), (n, α), (n, p) and (n, np) reactions. A simple power function $RS_n=aZ^b$ was very good to describe the systematics, where the parameters a and b were fitted according to the type of reactions. Most of the deviations between measured values and the systematic results are within a range of 25 %. Backward sputtering yields were lower by a factor of 1.5 to 180 than forward ones. The present results are discussed along with others experimental results and calculation results.

Keywords: Neutron Sputtering Yields, D-T Neutron, FNS, (n, 2n), (n, p), (n, α), (n, np), Fusion Reactor, Systematics

---

[※] On leave from University of Science and Technology of China

14.9MeV中性子によるスパッタリング率の系統的研究

日本原子力研究所東海研究所原子炉工学部
Bangjiao YE※・春日井好己・池田裕二郎

(1997年10月15日受理)

14.9MeV中性子により物質から放出される放射性核種のスパッタリング率(弾き出し率)を測定した。測定はF、Mg、Al、Sc、Ti、V、Cr、Fe、Co、Ni、Cu、Zr、Nb、Mo、Pd、Ag、Cd、In、Ta、Re、Pt、Au、Pb、SS316に対して行った。14.9MeV中性子の照射は、DT中性子源である原研FNS (Fusion Neutronics Source) を使って行った。弾き出され捕集膜に集められた物質の放射能を測定することで、捕集膜に集められた物質の量を算出した。照射は大気中で行った。スパッタリング率を調べるために、それぞれの試料に対して、試料と捕集膜との間を0.2、0.5、1.0、2.0、3.0、5.0mmとした。(n,2n)、(n,α)、(n,p)、(n,np) 反応を含む57反応についてスパッタリング率を測定した。(n,2n)、(n,α)、(n,p)、(n,np) 反応について、換算スパッタリング率 (RS_n) に対して、標的核の原子数 (Z) を関数とする系統性がわかった。その系統性は、簡単な経験式$RS_n = aZ^b$で表わすことができ、それぞれの反応について、フィッティングパラメータa、bを決めた。大部分の反応について、経験式は25%以下で測定値と一致した。前方スパッタリング率は後方に比べて1.5から180倍となった。今回の測定値を、その他の測定値または理論計算による値と比較した。

東海研究所:〒319-11 茨城県那珂郡東海村白方白根2-4
※外来研究員:中国科学技術大学

Contents

目　　次

1. Introduction

The development of materials for fusion reactors has been recognized as a fundamental issue affecting the ultimate technological and economic feasibility of fusion power. With the application of intense neutron fluxes in science, technology and power generation, the effects of high energy neutron bombardment, not only in the bulk material, but also at the surface become important. One of these surface effects is neutron sputtering, i.e., the removal of atoms (or clusters and microsize particles) from the surfaces during bombardment. It has been suggested that MeV neutron bombardment of the container walls of thermonuclear fusion reactors may lead to particle emission and cause both serious wall erosion and plasma contamination [1].

When energetic neutrons bombard a solid and the energy is transferred to a surface or a near-surface atom, sputtering can occur. There is a general physical interest in the neutron sputtering in connection with radiation damage [2] and ranges of energetic ions in solids [3]. Further, the neutron sputtering turned out to be an important process for emitting radioactive wall atoms into the coolants in nuclear reactors [4]. In fusion research, the neutron sputtering is of interest as being one of the mechanisms which introduce atoms from the solid wall of the plasma chamber into the hot deuterium-tritium plasma [5]. With the development of the fusion technology, especially for ongoing projects, e.g., the International Thermonuclear Experimental Reactor (ITER), the experimental data of the neutron sputtering yields should meet the needs for the basic material damage studies and the engineering design of fusion reactor.

Most of experimental measurements and theoretical treatments for neutron sputtering yields were carried out during the decade of 1970. After that time, there was almost no data in the literature on the fast neutron induced radioactivities recoil sputtering yields. Unfortunately, the neutron sputtering yields are still poorly investigated, mainly because the neutron fluences available are a factor of 10-100 lower than expected. The experimental data on the neutron sputtering yield is very scarce and contradictory. Different measurements on Nb, for example, had different results in widely scattering in the sputtering yields [6-8] and had large differences with the results predicted by theory [9-10]. Usually, the experimental data were much higher than the theoretical predictions [11-12]. The highest reported sputtering ratios have been associated with the observation of micron sized "chunks" of target material [5,8,13-17]. If the higher sputtering ratios were correct, neutron sputtering would be a critical issue for the fusion reactors.

The neutron sputtering yields, $S_n=Y/N$, have been reported by some research groups [6-7, 13,18-22], where Y is the number of atoms sputtered on a collector, and N is the total number of neutrons seen by the target. Since 1992, the researchers at the Fusion Neutronics Source (FNS) have started a systematic measurement for the neutron sputtering yields (S_n) by using the FNS facility. Y.Ikeda et al [23] have reported some results for S_n due to (n, 2n), (n, p) and (n, α) reactions in Al, Fe and Nb.

In this paper we report some new results for S_n by using the same facility and the same methods as that used by Y.Ikeda. Present measurements have been performed for S_n on 24 materials of F, Mg, Al, Sc, Ti, V, Cr, Fe, Co, Ni, Cu, Zr, Nb, Mo, Pd, Ag, Cd, In, Ta, Re, Pt, Au, Pb and SS316 with fifty-seven reactions. In order to examine a probable systematics for the forward sputtering yields, all S_n is reduced by corresponding cross section values, which is defined as a reduced sputtering yields (RS_n). A systematic study on RS_n as a function of the atomic number (Z) of the target materials for (n, 2n), (n, α), (n, p) and (n, np) reactions have been demonstrated. All present measurements were carried out by using collector positioned in air. On the one hand, due to the collision with air atoms, the sputtered atoms will attenuate passing through the air, which will lead to an incomplete collection of the sputtered atoms. Especially for high Z atoms, the range of the sputtered atoms is very short in air. For example, the range of the sputtered atom for ^{92}Nb with an average kinetic energy of 160 KeV in air was roughtly estimated to be 0.2 mm. In order to overcome this drawback, we need to measure the relation of the sputtering yields on the distances in air. Several different distances between the target and the collectors were chosen to be 0.2, 0.5, 1.0, 2.0, 3.0 and 5.0 mm. The sputtering yield in the surface of the target investigated (0 mm) was deduced from extrapolation of the sputtering yields at the different distances. On the other hand, with this method one can know the change of the sputtering yields along with the attenuation in air. Moreover, one can obtain some informations of the energy distribution of the sputtered atoms from the sputtering yields at different distances and the energy loss in air. Based on these reasons, we employed the sample configuration in the air.

2. Experimental procedures

2.1 Materials with reactions

The material released at a surface in the sputtering of solids by the neutron bombardment is mostly neutral atoms in the ground state, and only very few are emitted in the form of ions or small clusters [24]. For the neutron sputtering, the material released has been only little investigated. The most extensive sputtering yield measurements have been performed for Au [6,14, 25-29] and Nb [8, 13-14,30-36] materials.

Generally the neutron sputtering yields are very small, typically 10^{-5} to 10^{-4} atoms per incident neutron, of which 10^{-8} to 10^{-6} atoms per neutron are radioactive-primary-knockon atoms. Because the sputtering yields are very low, it is very important to select suitable materials and reactions. First, the cross section of the reaction must be not too low so that the

the FNS facility. Y.Ikeda et al [23] have reported some results for S_n due to (n, 2n), (n, p) and (n, α) reactions in Al, Fe and Nb.

In this paper we report some new results for S_n by using the same facility and the same methods as that used by Y.Ikeda. Present measurements have been performed for S_n on 24 materials of F, Mg, Al, Sc, Ti, V, Cr, Fe, Co, Ni, Cu, Zr, Nb, Mo, Pd, Ag, Cd, In, Ta, Re, Pt, Au, Pb and SS316 with fifty-seven reactions. In order to examine a probable systematics for the forward sputtering yields, all S_n is reduced by corresponding cross section values, which is defined as a reduced sputtering yields (RS_n). A systematic study on RS_n as a function of the atomic number (Z) of the target materials for (n, 2n), (n, α), (n, p) and (n, np) reactions have been demonstrated. All present measurements were carried out by using collector positioned in air. On the one hand, due to the collision with air atoms, the sputtered atoms will attenuate passing through the air, which will lead to an incomplete collection of the sputtered atoms. Especially for high Z atoms, the range of the sputtered atoms is very short in air. For example, the range of the sputtered atom for ^{92}Nb with an average kinetic energy of 160 KeV in air was roughtly estimated to be 0.2 mm. In order to overcome this drawback, we need to measure the relation of the sputtering yields on the distances in air. Several different distances between the target and the collectors were chosen to be 0.2, 0.5, 1.0, 2.0, 3.0 and 5.0 mm. The sputtering yield in the surface of the target investigated (0 mm) was deduced from extrapolation of the sputtering yields at the different distances. On the other hand, with this method one can know the change of the sputtering yields along with the attenuation in air. Moreover, one can obtain some informations of the energy distribution of the sputtered atoms from the sputtering yields at different distances and the energy loss in air. Based on these reasons, we employed the sample configuration in the air.

2. Experimental procedures

2.1 Materials with reactions

The material released at a surface in the sputtering of solids by the neutron bombardment is mostly neutral atoms in the ground state, and only very few are emitted in the form of ions or small clusters [24]. For the neutron sputtering, the material released has been only little investigated. The most extensive sputtering yield measurements have been performed for Au [6,14, 25-29] and Nb [8, 13-14,30-36] materials.

Generally the neutron sputtering yields are very small, typically 10^{-5} to 10^{-4} atoms per incident neutron, of which 10^{-8} to 10^{-6} atoms per neutron are radioactive-primary-knockon atoms. Because the sputtering yields are very low, it is very important to select suitable materials and reactions. First, the cross section of the reaction must be not too low so that the recoil atoms emitted can be detected. Second, the half-life of the reaction should be suitable so that the irradiation time and the time of measuring the activity of the collector foil can be sufficiently long . Third, the material should be solid with sufficiently smooth surface beacuse most of sputtering is caused from the surface layers. In four rounds experiments, twenty-four kinds of materials fluorine, magnesium, aluminium, scandium, titanium, vanadium, chromium, iron, cobalt, nickel, copper, zirconium, niobium, molybdenum, palladium, silver, cadmium, indium, tantalum, rhenium, platinum, gold, lead and stainless steel 316 with fifty-seven reactions were chosen for the measurement of the sputtering yields. All reactions and their associated decay data were listed in Tab.1.

2.2 Collector preparation

The sputtering yields have mostly been measured by subjecting a target material, each with collector foils on each side to a given neutron fluence in a vacuum. The present measurement was performed in air. For this method, it needs to measure the change of the activity at the collector with the distance between the target and the collector. The range of the sputtering atoms is very short because of attenuation by the air, which was very serious for high Z atom. In the present measurement, several different distances between the target and the collector were used to deduce the function of S_n varing with distances.

The collectors for the sputtering materials were made from the plastic film. Most of the collectors were first cut into a 2.5×2.5 cm^2 . The thickness of each collector is 0.013 mm . A plastic ring was made specially as a holder to fix the collector and the target. Each target-collector assembly consists of one target, two collectors and two plastic holders. The target was placed in between two holders. The collector was stuck on the other side of the holder relative to the target as shown in Fig.1. The thickness of the holder were 0.2, 0.5, 1.0, 2.0, 3.0 and 5.0 mm, which separated the target from the collectors. For each material investigated, 4 to 6 target-collector assemblies were prepared and were loaded into a cylinder plastic tube as a target-collector stack.

Though the method of the activation measurement of the collector has the advantage that any contamination on the collectors does not affect the measurements, the surface of the collectors should also be cleaned carefully, which will affect the sticking probability of the sputtering atoms on the collectors.

After irradiation, each collector was cut carefully into a round foil with 20 mm in diameter from the holder. Then, the activity of the collector was measured by Ge detectors.

2.3 Target preparation

For every experiment, the metallic target was used except fluorine. Most of samples were bought from the Goodfellow Cambridge Limited Company. The thickness of the target foils were from 0.005 mm to 0.25 mm as shown in Tab.2 and the size of target was 25×25 mm^2.

In order to perform well-defined sputtering measurements, the surfaces of the target to be investigated should be extremely carefully cleaned to avoid any surface debris or loosely bound microparticles being knocked off from the target and reaching the collectors. A surface layer of oxides, carbides, water and other residuals form will also influence the sputtering result.

2.4 D-T neutron source and sample irradiation

The 14.9 MeV neutrons were produced by T(d,n) reaction at the neutron generator of FNS. All measurements were carried out in four rounds experiments. Two rounds experiments were made at a rotational target room utilizing the FNS heavy irradiation machine time at an average neutron flux 2.2×10^{12} n/sec. Others two rounds experiments were made at a 80° target room at the average neutron flux 1.5×10^{11} n/sec. The target-collector stack was placed at the distances of 10 to 50 mm from the neutron source in direction of 0° to d^+ beam. The irradiation time was changed according to the half-lives of reactions. Excepting the ^{27}Al(n, p)^{27}Mg reaction for which the sample was only irradiated with 10 minutes, some samples were irradiated one day (about 7 to 10 hours), and other samples with long half-lives were irradiated two or three days (about 14 to 30 hours). A schematic of the irradiation configuration was shown in the Fig.1. The total neutron flux for each sample was given in Tab. 2.

2.5 Activity measurement

The material sputtered and deposited on the collectors is typically much less than 1/100 of a monolayer, therefore the most sensitive techniques had to be applied for a quantitative analysis. For that purpose, there are several techniques such as neutron activation analysis, nuclear track detectors [16] and surface analysis techniques[37-38], etc. In the present experiment, the activation analysis technique was used to determine the activity of the collector foils.

After the irradiations, the experimental target-collector stack was disassembled. The collector was cut carefully from the holder to avoid possible loss of sputtered material. Gamma-rays from the irradiated samples and the sputtered materials deposited in the collectors were measured using four germanium detectors. One germanium detector was used as the standard detector in which the detection efficiency in a standard position (5 cm from germanium detector) has been calibrated carefully. The other detectors were used to measure relative gamma-ray yields. The efficiencies of the relative detectors were calibrated for each gamma-ray peaks by measuring the same sample with both of the relative and the standard detectors.

The average neutron flux Φ_n on the sample can be obtained from gamma-ray peak counts C_1 of the sample

$$\Phi_n = \frac{C_1 \cdot \lambda \cdot F \cdot K}{I \cdot \sigma \cdot \varepsilon_1 \cdot n_1 \cdot \mu \cdot (1-e^{-\lambda t_{i1}})e^{-\lambda t_{c1}}(1-e^{-\lambda t_{m1}})} , \qquad (1)$$

where,

λ: decay constant of radioactivity produced,

σ: the cross section of reaction studied,

I: γ-ray emission probablity in a decay,

ε_1: the detector efficiency,

F : correction factor for non-constant neutron flux during irradiation,

K: coincidence-summing correction factor,

t_i: duration of irradiation,

t_c: duration of cooling,

t_m: duration of γ-ray counting,

n_1: the number of target nuclei of the sample,

μ : gamma-ray self-absorption correction factor.

The gamma-ray self-absorption correction factor , μ , is given by

$$\mu = \frac{(1-e^{-\rho t})}{\rho t} \quad , \qquad (2)$$

where ρ is the absorption coefficient (cm^{-1}) [39] and t is the thickness of the sample. For low energy gamma-ray and the thick target the self-absorption of the gamma-ray will become serious. For most samples this factor is larger than 0.98 as given in Tab. 2, only for Pd, Ta, Re, Pt and Pb samples the gamma-ray self-absorption correction factor are 0.75, 0.95, 0.90, 0.95 and 0.95, respectively.

The amount of sputtering is measured by the sputtering yield (S_n) which is defined as the mean number of atoms removed from the surface of a solid per neutron passing through this surface. In nearly all neutron sputtering measurements , a sticking probability of one was assumed. The γ-ray peak counts C_2 at the collector foil is

$$C_2 = \frac{S_n \cdot S_2 \cdot \Phi_n \cdot \varepsilon_2 \cdot I \cdot a \cdot (1-e^{-\lambda t_{i2}})e^{-\lambda t_{c2}}(1-e^{-\lambda t_{m2}})}{\lambda \cdot F \cdot K}, \tag{3}$$

where S_2 is the area of the collector foil measured, ε_2 is the detector efficiency. Substituting Φ_n in equation (1) to equation (3), considering n_1 equal to $WN_A a/A$, we get

$$S_n = \frac{C_2 \varepsilon_1 \sigma W N_A \mu}{C_1 \varepsilon_2 A S_2} e^{\lambda(t_{c2}-t_{c1})} \frac{(1-e^{-\lambda t_{m1}})}{(1-e^{-\lambda t_{m2}})}, \tag{4}$$

where W is the weight of the sample, A is the atomic weight of the target nuclide, a is the abundance of the target nuclide in the sample and N_A is the Avogadro's number (6.022045×10^{23}).

$\varepsilon_2 (E\gamma)$ can be obtained by measuring radioactivity of the same sample in two detectors, i.e., the standard detector and the relative detector. The efficiency curve $\varepsilon_1(E\gamma)$ in the standard detector has been calibrated. We have

$$\varepsilon_2(E_\gamma) = \frac{C_2'}{C_1'} K \varepsilon_1(E_\gamma) e^{\lambda(t_{c2}'-t_{c1}')} \frac{(1-e^{-\lambda t_{m1}'})}{(1-e^{-\lambda t_{m2}'})}. \tag{5}$$

Coincidence summing occurs for radionuclides emitting two or more photons in sequence within the resolving time of the spectrometer [40]. The probability for such summing effects increases with increasing total efficiency (ε_t). The coincidence-summing correction depend on the decay scheme. For a simple decay scheme as shown in Fig.2(a), if the p_1, p_2 and p_3, are emission probability of γ_1, γ_2 and γ_3, ε_1, ε_2 and ε_3 are the detection efficiencies for energies E_1, E_2 and E_3, ε_{t1} and ε_{t2} are full-energy-peak efficiencies at energies E_1 and E_2, respectively. We have

$$K = \begin{cases} \dfrac{1}{1-\varepsilon_{t2}} & , \text{ for } \gamma_1 \\ \dfrac{1}{1-p_1\varepsilon_{t1}/p_2} & , \text{ for } \gamma_2 \\ \dfrac{1}{1+\mathrm{p}_1\varepsilon_1\varepsilon_2/p_3\varepsilon_3} & , \text{ for } \gamma_3 \end{cases} \tag{6}$$

The correction factors become more complicated when more than two photons are emitted in cascade. If the decay scheme as shown in Fig.2(b), as an example, for detecting γ_1, such as 847 KeV gamma-rays measured for the $^{56}Fe(n,p)^{56}Mn$ reaction, the correction factor is

$$K = \frac{1}{1 - \frac{p_2}{p_1}\varepsilon_{t2} - \frac{p_3}{p_1}\varepsilon_{t3} - \frac{p_4}{p_1}\varepsilon_{t4}} \quad . \tag{7}$$

The results for the coincidence-summing correction factor for all reactions were given in Tab. 2.

3. Experimental results

The typical γ-ray spectra from the collectors for each sample were given in Figs. 3-33.

The neutron sputtering yields were obtained from the value of different positions for each sample for forward and backward directions, they were listed in Tab. 3 with their errors. The error consists of two parts: one is the statistial error for the peak count and another is all identified systematic error. All errors were listed as following:

ε_1 : 3%,
ε_2: depending on the errors of C_2, C_1, ε_1 (3 %) and K (3 %),
C_2 : peak counts error and statistial error,
C_1 : peak counts error and statistial error,
σ : depending on the reactions, about 3 % to 5 %,
n : WN_Aa/A , only weight W error, this is very small and can be neglected,
μ : can be neglected,
a : can be neglected,
S_2 : about 5 %.

The value of sputtering yields at 0 mm distance is obtained by extrapolating the data at different distances to 0 mm. The results were also given in Tab. 3. Figures.34-57 showed the fitting curves obtained from the sputtering yields of different distances for each target material. For most reactions the data of activity at the collector were measured more than three , but for some reactions such as ^{59}Co(n,p)^{59}Fe, ^{65}Cu(n,p)^{65}Ni, ^{90}Zr(n,p)^{90m}Y, ^{90}Zr(n,α)^{87m}Sr, ^{93}Nb(n,α)^{90m}Y for sample #1, ^{100}Mo(n,2n)^{99}Mo, ^{92}Mo(n,p)^{92m}Mo, ^{96}Mo(n,p)^{96}Nb, ^{108}Pd(n,α)^{105}Ru, ^{105}Pd(n,p)^{105}Rh, ^{110}Pd(n,2n)^{109}Pd, ^{107}Ag(n,2n)^{106m}Ag, ^{116}Cd(n,2n)^{115g}Cd, ^{112}Cd(n,p)^{112}Ag, ^{115}In(n,α)^{112}Ag, ^{115}In(n,2n)^{114m}In, ^{198}Pt(n,2n)^{197}Pt and ^{204}Pb(n,2n)^{203}Pb, only two data of the activities of the collectors were measured because of very weak activities. Some backward sputtering yields were also measured only for two distances because of the same reasons.

$$K = \frac{1}{1 - \frac{p_2}{p_1}\varepsilon_{t2} - \frac{p_3}{p_1}\varepsilon_{t3} - \frac{p_4}{p_1}\varepsilon_{t4}} \quad . \tag{7}$$

The results for the coincidence-summing correction factor for all reactions were given in Tab. 2.

3. Experimental results

The typical γ-ray spectra from the collectors for each sample were given in Figs. 3-33.

The neutron sputtering yields were obtained from the value of different positions for each sample for forward and backward directions, they were listed in Tab. 3 with their errors. The error consists of two parts: one is the statistial error for the peak count and another is all identified systematic error. All errors were listed as following:

ε_1 : 3%,
ε_2: depending on the errors of C_2, C_1 , ε_1 (3 %) and K (3 %),
C_2 : peak counts error and statistial error,
C_1 : peak counts error and statistial error,
σ : depending on the reactions, about 3 % to 5 %,
n : WN_Aa/A , only weight W error, this is very small and can be neglected,
μ : can be neglected,
a : can be neglected,
S_2 : about 5 %.

The value of sputtering yields at 0 mm distance is obtained by extrapolating the data at different distances to 0 mm. The results were also given in Tab. 3. Figures.34-57 showed the fitting curves obtained from the sputtering yields of different distances for each target material. For most reactions the data of activity at the collector were measured more than three , but for some reactions such as ^{59}Co(n,p)^{59}Fe, ^{65}Cu(n,p)^{65}Ni, ^{90}Zr(n,p)^{90m}Y, ^{90}Zr(n,α)^{87m}Sr, ^{93}Nb(n,α)^{90m}Y for sample #1, ^{100}Mo(n,2n)^{99}Mo, ^{92}Mo(n,p)^{92m}Mo, ^{96}Mo(n,p)^{96}Nb, ^{108}Pd(n,α)^{105}Ru, ^{105}Pd(n,p)^{105}Rh, ^{110}Pd(n,2n)^{109}Pd, ^{107}Ag(n,2n)^{106m}Ag, ^{116}Cd(n,2n)^{115g}Cd, ^{112}Cd(n,p)^{112}Ag, ^{115}In(n,α)^{112}Ag, ^{115}In(n,2n)^{114m}In, ^{198}Pt(n,2n)^{197}Pt and ^{204}Pb(n,2n)^{203}Pb, only two data of the activities of the collectors were measured because of very weak activities. Some backward sputtering yields were also measured only for two distances because of the same reasons.

4. Discussion

4.1 The systematics of the reduced sputtering yields

In order to give an overall guide line for S_n from a nuclear reaction point of view, S_n were reduced by using corresponding cross section values. We denoted the reduced sputtering yield as RS_n, that is,

$$RS_n = \frac{S_n}{\sigma(barn)} \quad . \tag{8}$$

In the present measurement, the experimental data of fifty-seven for RS_n have been classified according to their reaction types as (n, 2n), (n, α), (n, p) and (n, np). The reduced sputtering yields were plotted in Fig. 58 with respect to the atomic number (Z) of target materials for (n, 2n), (n, α), (n, p) and (n, np) reactions. In the Fig. 58 , we found that RS_ns present a strong correlation with Z. With the increasing of Z of the target materials, the values of RS_ns were decreased according to the power form of Z. The systematic trends of four reactions were similar. The RS_n dependence on Z is given in a very simple power function as following:

$$RS_n = a\,Z^{b} \quad , \tag{9}$$

where a and b are fitting parameters which are given in Tab. 4.

Following points is worth to be mentioned that for (n, np) reaction the data of the sputtering yields were obtained only for four reactions. The activity of ^{47}Sc comes from two reactions, i.e., ^{48}Ti(n,np)^{47}Sc and ^{47}Ti(n,p)^{47}Sc. For the natural target the abundance of ^{48}Ti is one order higher than that of ^{47}Ti, but the cross sections for the latter is larger than that of the former. The ratio of reaction rate between the ^{48}Ti(n,np)^{47}Sc and the ^{47}Ti(n,p)^{47}Sc is about 2:1. As an approximation we assume the activity of ^{47}Sc mainly coming from the ^{48}Ti(n,np)^{47}Sc reaction. For another reaction ^{52}Cr(n,2n)^{51}Cr, the activity of ^{51}Cr in SS316 target comes from two reactions, ^{52}Cr(n,2n)^{51}Cr and ^{54}Fe(n,α)^{51}Cr . The ratio of reaction rate between the former and the latter is about 6:1. So for the same reason we assume the activity of ^{51}Cr mainly coming from the ^{52}Cr(n,2n)^{51}Cr reaction.

Figure 62 showed the ratios of RS_n between the experimental values and the systematic values. For most of reactions, the experimental RS_n s were predicted by the systematics within 25 % error bands. Two reactions were exceptions, one was the ^{59}Co(n, α)^{56}Mn reaction which was 37 % larger than the systematics, and another was the ^{52}Cr(n,2n)^{51}Cr reaction which was 57 % larger than the systematics. It also needs to point out that for the

$^{52}Cr(n,2n)^{51}Cr$ reaction the target was supported by a polyester support. For the same reaction using SS316 target the result was in good agreement with the systematics. In addition, it needs to keep in mind that for all sputtering experiment, the sticking probability was supposed to be one, although the sticking probability would be changed slightly depending on the collector materials and the sputtered atoms[41].

In order to confirm the experimental results, the sputtering yields for six samples of niobium, palladium, silver, cadmium, indium and gold were measured in twice. Except niobium sample, both of which were irradiated at the rotational target room, for other five samples, the first time was irradiated at the 80° target room and the second one was irradiated at the rotational target room. Both of the results for $^{116}Cd(n,2n)^{115g}Cd$, $^{110}Pd(n,2n)^{109}Pd$ and $^{115}In(n,2n)^{114}In$ reactions were almost the same. For $^{93}Nb(n, 2n)^{92m}Nb$, $^{93}Nb(n,\alpha)^{89m}Y$, $^{107}Ag(n,2n)^{106m}Ag$ and $^{197}Au(n,2n)^{196g}Au$ reactions both of the results showed a little differences, but both results were in agreement with the systematics within 25 % error bands.

4.2 Backward sputtering yields

Because neutrons can penetrate through a solid with large thickness , we have to distinguish between the backward sputtering and the forward sputtering. The greater forward compared with the backward sputtering yield for energetic neutrons, is caused by the isotropic scattering which strongly favours energy transfer in the forward direction [24]. In the present measurement, the backward sputtering yields for thirteen reactions heve been measured. The backward sputtering yields are lower by a factor of 1.5 to 200 than the forward sputtering yields depending on the target materials as shown in Tab.3. For $^{19}F(n,2n)^{18}F$ reaction we found the backward sputtering yields was very large. The ratios F/B of S_n between the forward and the backward was 1.5. Except this reaction, we can postulate that the ratio F/B depends on reaction types, for example, 80-180 for (n, p) reaction, 30-120 for (n, 2n) reaction and 5-20 for (n, α) reaction.

4.3 Comparison with other experimental results

At 1970's and the begining of 1980's some experimental groups have made some measurements on the neutron sputtering yields for some materials as Au, Nb, Al, Fe, V , Mo , Cr , Ni and Co . Most of experimental study on the neutron sputtering is focused on Nb and Au, with the neutron sources for reactor neutrons as well as neutrons from a T(d,n) and a Be(d,n) neutron sources. The measurements have been made by measuring the amount of deposition on a collector foil assuming a sticking probability equal to 1. In most cases polycrystalline targets were used at room temperature in a vacuum condition. Sputtering yields data of experiments with single crystals on Nb and Au [15, 27, 32] agreed within the experimental error. Most reliable measurements are made with $S_n < 10^{-5}$ as only upper limits. Microparticles or chunks have been found on the collectors by two experimental groups in sputtering rough surfaces contribution less than 10% to the total sputtering yield [15,24]. Present results were compared with the results of Y.Ikeda [23], M.Thomas [42], R.Behrisch [43] and O.K.Harling [4] as shown in Tab.5.

4.3.1 (n,2n) reaction

For (n,2n) reaction, except for M.Thomas' results, most of other experimental results were larger than the present results as shown in Fig.59. The sputtering yields for twenty-nine reactions have been measured for atomic number Z from 9 to 82 in the present experiment . Many results of the neutron sputtering yields were obtained for the first time in the world, for example, $^{19}F(n,2n)^{18}F$, $^{45}Sc(n,2n)^{44m}Sc$, $^{59}Co(n,2n)^{58}Co$, $^{65}Cu(n,2n)^{64}Cu$, $^{90}Zr(n,2n)^{89}Zr$, $^{110}Pd(n,2n)^{109}Pd$, $^{102}Pd(n,2n)^{101}Pd$, $^{107}Ag(n,2n)^{106m}Ag$, $^{116}Cd(n,2n)^{115g}Cd$, $^{115}In(n,2n)^{114}In$, $^{181}Ta(n,2n)^{180m}Ta$, $^{187}Re(n,2n)^{186}Re$, $^{196}Pt(n,2n)^{195}Pt$, $^{198}Pt(n,2n)^{197}Pt$ and $^{204}Pb(n,2n)^{203}Pb$ reactions. For $^{93}Nb(n,2n)^{92m}Nb$ reaction, M.T.Thomas et al using (d,t) neutron gave the $RS_n=2.28 \times 10^{-7}$ barn^{-1} with the total neutron dose 3×10^{16}, O.Harling gave $RS_n=1.58\times10^{-7}$ barn^{-1} , R.Behrisch gave $RS_n=1.70\times10^{-7}$ barn^{-1} and Y.Ikeda gave $RS_n=2.5\times10^{-7}$ barn^{-1} . The present results were $RS_n=5.73\times10^{-8}$ barn^{-1} and 4.48×10^{-8} barn^{-1}, which were about 3-5 times lower than other results. For $^{197}Au(n,2n)^{196g}Au$ reaction, O.Harling gave $RS_n=5.5\times10^{-8}$ barn^{-1} , R.Behrisch gave $RS_n=1.10\times10^{-7}$ barn^{-1} and Y.Ikeda gave $RS_n=6.0\times10^{-8}$ barn^{-1} . The present result was $RS_n=6.53\times10^{-9}$ barn^{-1} which was about one order lower than Ikeda's result and about 17 times lower than Behrisch's result. Thomas' results for $^{58}Ni(n, 2n)^{57}Ni$, $^{100}Mo(n,2n)^{99}Mo$, $SS316(n,2n)^{51}Cr$ and $SS316(n,2n)^{57}Ni$ reactions were about 2-3 times lower than the present results.

4.3.2 (n,p) reaction

For (n,p) reaction, the discrepancies among the experimental results of three groups, i.e., Y.Ikeda, M.Thomas and O.Harling, as shown in Fig.60, were very large. Present results for $^{24}Mg(n,p)^{24}Na$, $^{27}Al(n,p)^{27}Mg$, $^{59}Co(n,p)^{59}Fe$, $^{65}Cu(n,p)^{65}Ni$, $^{90}Zr(n,p)^{90m}Y$, $^{105}Pd(n,p)^{105}Rh$, $^{112}Cd(n,p)^{112}Ag$ and $SS316(n,p)^{56}Mn$ reactions were obtained for the first time in the world. For the same target nickel, the reduced sputtering yield for two reactions: $^{58}Ni(n,p)^{58}Co$ and $^{60}Ni(n,p)^{60}Co$, should be the same value according to the present systematics beacuse their atomic number Z is the same. Y.Ikeda gave approximately equal results for both reactions. For the former reaction M.thomas gave a 3.5 times larger value than that of the latter and also O.Harling gave 3 times value. It is unable to explain from our present systematics why so much different values were reported in the reduced sputtering yields for the same Z. Another example is Mo sample for 4 kinds of (n,p) reactions. In the present work, two reactions: $^{92}Mo(n,p)^{92m}Nb$ and $^{96}Mo(n,p)^{96}Nb$ have been measured with almost the same values. M.Thomas has reported all these reactions having very large different values in each. The value of reduced sputtering yield for the $^{96}Mo(n,p)^{96}Nb$ was two orders larger than that of the $^{95}Mo(n,p)^{95m}Nb$ reaction. For the same reaction, such as, $^{60}Ni(n,p)^{60}Co$ reaction, the maximum disparity between Y.Ikeda's and M.Thomas' values was about 35 times. For the $^{56}Fe(n,p)^{56}Mn$ reaction, the present result was the same with Y.Ikeda within the experimental error, but was 4 times larger than that of O.Harling. For the $^{48}Ti(n,p)^{48}Sc$ reaction, the present result was in good agreement with O.Harling's within the experimental error.

4.3.3 (n, α) reaction

For (n,α) reaction, the experimental results of two groups Y.Ikeda and O.Harling were shown in Fig.61. The present results for $^{45}Sc(n, \alpha)^{42}K$, $^{59}Co(n, \alpha)^{56}Mn$, $^{90}Zr(n, \alpha)^{87m}Sr$, $^{92}Mo(n, \alpha)^{89m+g}Zr$, $^{108}Pd(n, \alpha)^{105}Ru$ and $^{115}In(n, \alpha)^{112}Ag$ reactions were newly obtained. For the $^{27}Al(n, \alpha)^{24}Na$ reaction, the present result was in good agreement with Y.Ikeda's result. For the $^{93}Nb(n, \alpha)^{90m}Y$ reaction, Y.Ikeda's result was higher about 4 times than the present results. For the $^{51}V(n, \alpha)^{48}Sc$ reaction, the differences for three experimental results were small. For the $^{50}V(n, \alpha)^{47}Sc$ reaction, O.K.Harling's result was about 3 orders lower than the present systematics, and for the $^{50}Ti(n, \alpha)^{47}Ca$, the $^{54}Fe(n, \alpha)^{51}Cr$ and the $^{62}Ni(n, \alpha)^{59}Fe$ reactions, O.K.Harling's results were about one order lower than the present systematics.

4.3.4 (n, np) reaction

For (n, np) reaction, only one experimental result: SS316(n, np)^{57}Co reaction, was given before our experiment by M.Thomas with $RS_n=7.56\times10^{-8}$ barn^{-1} which was one order lower than the present result. The present results for $^{48}Ti(n, np)^{47}Sc$ and $^{102}Pd(n, np)^{101m}Rh$ reactions were newly obtained. According to the scarcity of the arailable data for (n, np) reaction, present systematics for this reaction only gave a rough result.

4.4 Theoretical considerations

Sputtering processes can generally be described using the concepts developed for radiation damage in the bulk of a material [2,44-48]. An incident neutron interacts with an atom of the solid and it produces an energetic primary knockon atom with energy *T*. These primary atoms collide further with lattice atoms and/or with electrons and making up a collision cascade. If a primary knockon atom and a collision cascade are initiated in the near-surface layers of the solid, energetic atoms may reach the surface and can be released. The sputtering yield is derived as the mean number of cascade atoms per incident neutron which reach the surface with sufficient energy to overcome the surface potential, which is of the order of 2-10 eV [49].

In sputtering experiments with neutrons, the primary knockon atoms can be produced in a nuclear reaction such as (n, p), (n, α), (n, 2n), (n,np), etc. Inelastic scattering refers to those events in which a particle is emitted, leaving the residual nucleus in an excited state which decays by photo emission [50]. The recoil energy T is

$$T = (1 - 2\mu f + f^2)\frac{T_m}{4} \quad , \tag{10}$$

where

$$f = \sqrt{1 - \frac{(1+A_1)Q}{A_1 E_n}} \quad , \tag{11}$$

where E_n is the incident neutron energy, Q is the inelastic excitation of the nucleus, A_1 is the target mass, $\mu = cos\theta$ and θ is the scattering angle, and the maximum transfered energy T_m is

$$T_m = \frac{4A_1 E_n}{(1+A_1)^2} \quad . \tag{12}$$

The radioactive primary knockon atoms starting with an energy T in the direction θ of the neutron may have a range distribution $F_R(T,\theta,x)dx$ in the direction x normal to the surface. If they start, which are uniformly distributed, in the solid of thickness c at distances x_0 from the surface, the probability for an atom to reach the surface and be emitted is given by

$$\int_0^c dx_0 \int_0^\infty F_R(T,\theta,x+x_0)dx \ .$$

If the thickness c is much larger than the mean range, this can be transformed to

$$\int_0^\infty x F_R(T,\theta,x+x_0)dx \ ,$$

here the surface potential is neglected, because we assume that the majority of the atoms arrive at the surface with much higher energies.

The primary knockon emission yields in the forward directions are given by [51-53]

$$S_{n,f}(E_n,\theta)=\frac{N}{\cos\theta}\sigma(E_n)\int_0^{\infty}xF_R(T,\theta,x)dx\ , \tag{13}$$

where $\sigma(E_n)$ is the cross section of reaction between the incoming neutron and the atoms in the solid, N is the number density of atoms in the solid . The mean projected range of a primary knockon atom starting with T in a solid in a direction θ relative to the surface normal, given by

$$\langle R(T,\theta)\rangle=\frac{\int_0^{\infty}xF_R(T,\theta,x)dx}{\int_0^{\infty}F_R(T,\theta,x)dx}\ . \tag{14}$$

For nearly perpendicular neutron incidence ($\theta=0$), the denominator is close to 1. For single-energy neutrons we get for the forward emission yield of radioactive primary knockon atoms

$$S_{n,f}=K\sigma(E_n)N\langle R(T)\rangle\quad , \tag{15}$$

where K was introduced as an adjustable paremeter depends on the geometry, the surface binding energy of the target material and the direction of the neutron flux.

Using average kinetic energy $T=T_m/4$, the theoretical mean ranges have been calculated using the results of Schiott [56] for the low and intermediate energy ranges.

$$\langle R(T)\rangle\ (\frac{\mu g}{cm^2})=\begin{cases}C_l A_2(\frac{Z_1^{2/3}+Z_2^{2/3}}{Z_1Z_2}T(keV))^{2/3}, & \varepsilon<0.1\\ C_i A_2\frac{(Z_1^{2/3}+Z_2^{2/3})^{1/2}}{Z_1Z_2}T(keV)\ , & 0.5<\varepsilon<10\end{cases}\quad , \tag{16}$$

where

$$\varepsilon=\frac{32.5A_2}{(A_1+A_2)Z_1Z_2(Z_1^{2/3}+Z_2^{2/3})^{1/2}}T(keV)\quad , \tag{17}$$

where A_1, Z_1 and A_2, Z_2 are the atomic masses and the atomic numbers of the target atoms and the recoil atoms, respectively, ε is defined as a reduced energy, and C_l and C_i are obtained from Fig.4 and 7 of Schiott [54].

The calculated results are given in Tab.6 with K=1. The kinetic energies of the residual nucleus are varies from 700 KeV to 70 KeV with atomic number from 9 to 82. The maximum mean range is about 2 μm for fluorine and the value decreases with increasing Z. The comparison between the calculated results and the experimental results are also given in Tab.6. The ratios C/E changes with Z depending to the type of reaction are given in Fig.63. The result shows that the ratios C/E varies from 0.5 to 5 depending on the type of reactions. For the same material, according to the present systematics, (n,α) reaction gives the largest the reduced sputtering yield and (n,2n) gives the lowest ones (for example, the ratio of the reduced sputtering yields (n,2n) to (n,α) reactions is 0.36 for Z=20 and 0.13 for Z=100) in the reactions considered. This cann't be explained by the present sputtering theory. In order to explain the systematics of RS_n, it is necessary to develop a new neutron sputtering theory.

5. Summary and conclusion

We made a systematic study on the neutron sputtering yields. Twenty-four kinds of materials have been chosen for sputtering experiments at the neutron energy 14.9 MeV using FNS D-T neutron facility. The present work was made to provide experimental data of the sputtering yields induced by 14 MeV neutrons. In the present work, the data of twenty-nine (n, 2n) reactions for Z from 9 to 82, ten (n, α) reactions for Z from 13 to 49, fourteen (n, p) reactions for Z from 12 to 48, and four (n, np) reactions for Z from 22 to 46 were measured. The neutron sputtering was characterized by the reduced sputtering yield which depends strongly on the atomic number Z of target materials. A simple power function was very good to describe the systematics. For most of reactions, the experimental RS_n s were predicted by the systematics within 25 % error bands. Backward sputtering yields of thirteen reactions also have been measured, which was lower by a factor of 1.5 to 180 than forward one.

Further, from the present systematics, one can deduce the sputtering yields for some important materials, especially for those the recoil nuclides with no activities. In a fusion power reactor, for example, ITER, the first wall are bombarded with a high flux 14 MeV neutrons and wall material particles are sputtered back to the plasma. In addition to the effects on the plasma, this process results in the cause of wall erosion. A material with a large erosion rate should be avoided as a candidate for the material of the first wall. The erosion rates of the candidate materials, such as vanadium-base alloys, can be estimated from our systematics. Moreover, the radioactive nuclides sputtered from the first wall into the coolant, mainly come from the non-elastic reaction, can be calculated from the present work.

The present systematics, however, cann't be explained well by the theory at the present moment. The sputtering theory will be developed based on the present systematics.

comparison between the calculated results and the experimental results are also given in Tab.6. The ratios C/E changes with Z depending to the type of reaction are given in Fig.63. The result shows that the ratios C/E varies from 0.5 to 5 depending on the type of reactions. For the same material, according to the present systematics, (n,α) reaction gives the largest the reduced sputtering yield and (n,2n) gives the lowest ones (for example, the ratio of the reduced sputtering yields (n,2n) to (n,α) reactions is 0.36 for Z=20 and 0.13 for Z=100) in the reactions considered. This cann't be explained by the present sputtering theory. In order to explain the systematics of RS_n, it is necessary to develop a new neutron sputtering theory.

5. Summary and conclusion

We made a systematic study on the neutron sputtering yields. Twenty-four kinds of materials have been chosen for sputtering experiments at the neutron energy 14.9 MeV using FNS D-T neutron facility. The present work was made to provide experimental data of the sputtering yields induced by 14 MeV neutrons. In the present work, the data of twenty-nine (n, 2n) reactions for Z from 9 to 82, ten (n, α) reactions for Z from 13 to 49, fourteen (n, p) reactions for Z from 12 to 48, and four (n, np) reactions for Z from 22 to 46 were measured. The neutron sputtering was characterized by the reduced sputtering yield which depends strongly on the atomic number Z of target materials. A simple power function was very good to describe the systematics. For most of reactions, the experimental RS_n s were predicted by the systematics within 25 % error bands. Backward sputtering yields of thirteen reactions also have been measured, which was lower by a factor of 1.5 to 180 than forward one.

Further, from the present systematics, one can deduce the sputtering yields for some important materials, especially for those the recoil nuclides with no activities. In a fusion power reactor, for example, ITER, the first wall are bombarded with a high flux 14 MeV neutrons and wall material particles are sputtered back to the plasma. In addition to the effects on the plasma, this process results in the cause of wall erosion. A material with a large erosion rate should be avoided as a candidate for the material of the first wall. The erosion rates of the candidate materials, such as vanadium-base alloys, can be estimated from our systematics. Moreover, the radioactive nuclides sputtered from the first wall into the coolant, mainly come from the non-elastic reaction, can be calculated from the present work.

The present systematics, however, cann't be explained well by the theory at the present moment. The sputtering theory will be developed based on the present systematics.

Acknowledgments

The authors gratefully acknowledge the staffs of FNS for their support and help during the experiment. They also thank C.Kutsukake, S.Tanaka, Y.Abe and other members of Division of Reactor Physics Facilities for operation of the FNS accelerator.

References

1) Kaminsky M.: IEEE Trans.Nucl.Sci. NS , 18, 208(1971).
2) Sigmund P.: Phys. Rev., 184, 383(1969).
3) Biersack J.: Z.Phys., 211, 495(1968).
4) Harling O.K., et al.: J.Appl.Phys., 48, 4328(1977).
5) Behrisch R., et al.: J.Appl.Phys., 48, 3914(1977).
6) Behrisch R., et al.: J. Nucl. Mater., 53, 183(1974).
7) Jenkins L.H., et al.: J. Nucl.Mater. 63, 438(1976).
8) Kaminsky M., et al.: J. Nucl. Mater. 53, 162(1974).
9) Baer T.S. and Anno J.N.: J.Appl.Phys. 43, 2453(1972).
10) Behrisch R.: Nucl. Fusion, 12, 695(1972).
11) Robinson M.T.: J.Nucl. Mater. 53, 201(1974).
12) Behrisch R.: Nucl.Instr.Meth. 132, 293(1976).
13) Kaminsky M., et al.: Phys.Rev. Lett. 32, 599(1974).
14) Harling O.K., et al.: Phys. Rev. Lett. 34, 1340(1975).
15) Kaminsky M., et al.: J.Nucl.Mater. 60, 111(1976).
16) Biersack J., et al.: J.Nucl.Mater. 53, 194(1974).
17) Robinson J.E., et al.: J.Nucl.Mater., 63, 432(1976).
18) Norcross D.W., et al.: J.Appl.Phys. 37, 621(1966).
19) Logan C.M., et al., J.Vac.Sci. Technol. 12(1975)536.
20) Rohinson J.E. and Thompson D.A.: Phys.Rev.Lett. 33, 1569(1974).
21) Meisenheimer R.G.: J.Vac.Sci.Technol. 14, 560(1977).
22) Harling O.K., et al.: J. Nucl. Mater. 63, 422(1976).
23) Ikeda Y. and Konno C.: JAERI-M, 93-046, 316(1993).
24) Behrisch R. (ed.): Sputtering by Particle Bombardment II, pp196, (Springer-Verlag, Berlin, Heidelberg, Now York, Tokyo 1983).
25) Keller K.: Plasma Phys. 10, 195(1968).
26) Verghese K.: Trans.Am.Nucl.Soc. 12, 544(1969).
27) Kirk M.K., et al.: Phys.Rev. B19, 87(1979).
28) Kirk M.K., et al.: J.Nucl. Mater.53, 179(1974).
29) Keller K. and Lee R.V.: J.Appl. Phys. 37, 1890(1966).
30) Dusza D., et al.: In Radiation Effects on Solid Surface, Ed. by Kaminsky M., Advances in Chemistry Series, No.158, (The American Chemical Society 1976).
31) Rose D.J.: Nucl.Fusion, 9, 183(1969).
32) Harling O.K., et al.: J.Appl.Phys. 48, 4315(1977).
33) Biersack J., et al.: J.Nucl.Mater. 63, 443(1976).

34) Jenkins L.H., et al.: Appl.Phys. Lett. 26, 426(1975).
35) Jenkins L.H., et al.: J.Nucl.Mater. 63, 438(1976).
36) Meisenheimer R.G. :J. Nucl. Mater. 63, 429(1976).
37) Czanderna A.W. (ed.): Methods of Surface Analysis, Vol.1 (Elsevier, Amsterdam 1975).
38) Benninghoven A., et al. (ed.): Secondary Ion Mass Spectrometry, SIMS III, (Springer, Berlin, Heidelberg, New York 1982).
39) Storm E., et al.: Nucl. Data Tables, A7, 565(1970).
40) Debertin K. and Helmer R.G.: Gamma-ray and x-ray Spectrometry with Semiconductor Detectors., p259.
41) Emmoth B. and Bergsaker K.: Nucl. Instr. Meth. B33, 435(1988).
42) Thomas M.T., et al.: J. Nucl.Mater. 63, 448(1976).
43) Behrisch R., et al.: J.ucl.Mater. 108, 73(1982).
44) Nelson R.S.: The Observation of Atomic Collisions in Crystalline Solids (North-Holland, Amsterdam 1968).
45) Thompson M.W., Nelson R.S.: Philos. Mag. 7, 2015(1962).
46) Robinson M.T.: Philos. Mag. 12, 145,741(1965).
47) Thompson M.W.: Defects and Radiation Damage in Metals, (University Press, Cambridge 1969).
48) Sigmund P.: Rev. Roum. Phys. 17, 823, 969(1972).
49) Behrisch R. (ed.): Sputtering by Particle Bombardment I, Topics Appl. Phys., Vol.47, Chaps.2,3. (Springer, Berlin, Heidelberg, Now York 1981).
50) Robinson M.T.: Radiation Damage in Metals, ed. by Peterson N.L., et al., (Amer.Soc.Metals, Metals Park, Ohio 1976)pp.1-57.
51) Robinson M.T. : In Nucl. Fusion Reactors (Brit. Nucl. Energy Society, London 1970).
52) Roberto J.B., et al.: J.Nucl.Mater. 63, 460(1976).
53) Klabunde C.E., et al.: J.Nucl.Mater. 108 109, 21(1982).
54) Schott H.E.: Radiation Effects, 6, 107(1970).
55) Ikeda Y., et al.: JAERI-1312, (1988).
56) Konno C., et al.: JAERI-1329, (1993).
57) Victoria M., (ed.) et al.: Neutron Cross Sections, Vol.2, Academic press, INC.(1988).

Table 1 List of reactions and associated decay data for the neutron sputtering experiment

Z	Reactions	Abundance (%)	$T_{1/2}$	Energy (keV)	Branching ratio (%)	$\sigma^{\#}$ (mb)	Q-values* (MeV)
9	^{19}F (n,2n) ^{18}F	100	1.83h	511	193.8	51.8	-10.43
12	^{24}Mg (n,p) ^{24}Na	78.99	15.03h	1368	100	167.6	-4.73
13	^{27}Al (n,α) ^{24}Na	100	15.03h	1368	100	113.9	-3.13
	(n,p) ^{27}Mg	100	9.46m	843.7	73.1	62.3	-1.83
21	^{45}Sc (n,α) ^{42}K	100	12.4h	1524	18.8	53.3	-0.4
	(n,2n) ^{44m}Sc	100	2.44d	271	86.6	131	-11.32
22	^{47}Ti (n,p) ^{47}Sc	7.4	3.422d	159.4	68.5	121.5	0.18
	^{48}Ti (n,p) ^{48}Sc	73.7	43.67h	983.5	100	59.6	-3.21
	(n,np) ^{47}Sc	73.7	3.422d	159.4	68.5	20.7	-11.44
23	^{51}V (n,α) ^{48}Sc	99.75	43.67h	983	100	16.9	-2.06
24	^{52}Cr (n,2n) ^{51}Cr	83.79	27.7d	320	10.2	376	-12.04
26	^{56}Fe (n,p) ^{56}Mn	91.8	2.58h	847	98.9	111	-2.91
27	^{59}Co (n,α) ^{56}Mn	100	2.579h	846.7	98.9	32.3	0.33
	(n,2n) ^{58}Co	100	70.8d	811	99.4	630	-10.45
	(n,p) ^{59}Fe	100	44.5d	1099	56.5	45.7	-0.78
28	^{58}Ni (n,p) ^{58}Co	68.3	70.8d	811	99.4	269	0.4
	(n,2n) ^{57}Ni	68.3	35.99h	1377.6	77.6	42	-12.2
	(n,np) ^{57}Co	68.3	271.65d	122.06	85.6	661	-8.17
29	^{65}Cu (n,2n) ^{64}Cu	30.8	12.7h	511	38.6	961	-9.91
	(n,p) ^{65}Ni	30.8	2.52h	1115.8	15.13	18.8	-1.35
40	^{90}Zr (n,p) ^{90m}Y	51.5	3.19h	479	91	12.28	-1.5
	(n,α) ^{87m}Sr	51.5	2.81h	388.4	87	3.82	1.76
	(n,2n) ^{89}Zr	51.5	78.4h	909	99	832	-11.98
41	^{93}Nb (n,α) ^{90m}Y	100	3.19h	479	91	4.94	4.93
	(n,2n) ^{92m}Nb	100	10.15d	934	99	464	-8.83
42	^{92}Mo (n,p) ^{92m}Nb	14.8	10.14d	934.5	99.2	58.8	0.43
	(n,α) $^{89m+g}$Zr	14.8	78.43h	909.2	99	25.6	3.71
	^{96}Mo (n,p) ^{96}Nb	16.7	23.55h	778.2	96.8	24.7	-2.4
	^{100}Mo (n,2n) ^{99}Mo	9.6	66.02h	739.4	12.6	1380	-8.29
46	^{102}Pd (n,2n) ^{101}Pd	1	8.47h	296.3	18	1179	-10.57
	^{102}Pd (n,np) ^{101m}Rh	1	4.34d	306.77	87	270	-7.81
	^{110}Pd (n,2n) ^{109}Pd	11.8	13.43h	88	96	1550**	-8.82
	^{105}Pd (n,p) ^{105}Rh	22.2	1.47d	319.1	19.7	42.7	0.22
	^{108}Pd (n,α) ^{105}Ru	26.7	4.44h	724.2	17.8	3.33	2.05

Table 1 (continued-1)

Z	Reactions			Abundance (%)	$T_{1/2}$	Energy (keV)	Branching ratio (%)	$\sigma^{\#}$ (mb)	Q-values* (MeV)
47	^{107}Ag	(n,2n)	^{106m}Ag	51.83	8.41d	450	28.4	557	-9.54
48	^{116}Cd	(n,2n)	^{115g}Cd	7.5	55.38h	336	95	780**	-8.7
	^{112}Cd	(n,p)	^{112}Ag	24.1	3.14h	617.3	42	18.1	-3.17
49	^{115}In	(n,2n)	^{114m}In	95.7	49.51d	190	95.6	1255**	-9.04
		(n,α)	^{112}Ag	95.7	3.14h	617.6	42	2.66	2.73
73	^{181}Ta	(n,2n)	^{180m}Ta	100	8h	93	5	1297	-7.58
75	^{187}Re	(n,2n)	^{186}Re	62.6	3.78d	137	9.2	1560**	-7.36
78	^{196}Pt	(n,2n)	^{195}Pt	25.3	4.02d	98.9	100	1692+	-7.92
	^{198}Pt	(n,2n)	^{197}Pt	7.2	18.3h	191	16	1100**	-7.56
79	^{197}Au	(n,2n)	^{196g}Au	100	6.2d	355.65	87.6	1894	-8.07
			^{196m}Au	100	9.7h	188.23	37.8	1300	-8.07
82	^{204}Pb	(n,2n)	^{203}Pb	1.42	52.02h	279.2	81	2120	-8.39
SS 316	^{56}Fe	(n,p)	^{56}Mn	~59.3	2.58h	846.75	98.9	111	-2.91
	^{52}Cr	(n,2n)	^{51}Cr	~14.4	27.7d	320	10.2	376	-12.04
	^{58}Ni	(n,p)	^{58}Co	~9.6	70.8d	811	99.4	269	0.4
		(n,np)	^{57}Co	~9.6	271.65d	122	85.6	661	-8.17
		(n,2n)	^{57}Ni	~9.6	35.99h	1377.6	77.6	42	-12.2

\# : Data were taken from Refs. 55 and 56.

* : E_n=14.9 MeV, Qtool (T-2 Nuclear Information Service in the Internet) was used to calculate reaction Q-values.

** : Data were taken from Ref.57.

\+ : The cross section was calculated using the systematic formula at Ref.56.

Table 2 List of neutron flux and correction factors for the sputtering experiment

Z	Reactions	Energy (keV)	Thickness of target (mm)	Neutron flux Total ($x10^{16}$)	Neutron flux Average ($x10^{12}$/s)	Correction factors K	Correction factors μ
9	^{19}F (n,2n) ^{18}F	511	0.1	3.44	2.5	1	0.9994
12	^{24}Mg (n,p) ^{24}Na	1368.6	0.1	6.92	2.3	1.062	0.9996
13	^{27}Al (n,α) ^{24}Na	1368.6	0.1	8.09	2.4	1.062	0.9993
	(n,p) ^{27}Mg	843.8	0.1	0.0093	0.16	1.001	0.9972
		1014				0.999	0.9992
21	^{45}Sc (n,α) ^{42}K	1524	0.025	0.394	0.19	1	0.9998
	(n,2n) ^{44m}Sc	271	0.25*			1	0.996
22	^{47}Ti (n,p) ^{47}Sc	983.5	0.1	0.871	0.16	1	0.9986
	^{48}Ti (n,p) ^{48}Sc	1037				1.006	0.9987
	(n,np) ^{47}Sc	159.4				1	0.9963
23	^{51}V (n,α) ^{48}Sc	983.5	0.025	0.429	0.17	1	0.9997
24	^{52}Cr (n,2n) ^{51}Cr	320	0.015**	14.18	1.9	1	0.9994
26	^{56}Fe (n,p) ^{56}Mn	846.75	0.1	8.22	2.3	1.037	0.9974
27	^{59}Co (n,α) ^{56}Mn	846.75	0.02	0.809	0.16	1.037	0.9994
	(n,2n) ^{58}Co	810.76				1	0.9994
	(n,p) ^{59}Fe	1099				1.005	0.9995
28	^{58}Ni (n,p) ^{58}Co	810.76	0.1	0.789	0.13	1	0.9969
	(n,2n) ^{57}Ni	1377.6				1	0.9978
	(n,np) ^{57}Co	122.06				1.036	0.9829
29	^{65}Cu (n,2n) ^{64}Cu	511	0.02	8.23	2.4	1	0.9993
	(n,p) ^{65}Ni	1115.8				1.044	0.9995
40	^{90}Zr (n,p) ^{90m}Y	479.51	0.02	7.92	2.2	1	0.9994
	(n,α) ^{87m}Sr	388.4				1.078	0.9993
	(n,2n) ^{89}Zr	909.2				1	0.9996
41, #1	^{93}Nb (n,α) ^{90m}Y	479.51	0.025	15.4	2.3	1	0.9988
	(n,2n) ^{92m}Nb	934.51				1.076	0.9992
41, #2	^{93}Nb (n,α) ^{90m}Y	479.51	0.025	15.5	2.2	1	0.9988
	(n,2n) ^{92m}Nb	934.51				1.076	0.9992
42	^{92}Mo (n,p) ^{92m}Nb	934.51	0.015	15.28	2.5	1.076	0.9995
	(n,α) $^{89m+g}Zr$	909.2				1	0.9995
	^{96}Mo (n,p) ^{96}Nb	778.2				1	0.9995
	^{100}Mo (n,2n) ^{99}Mo	739.4				1	0.9995
46, #1	^{110}Pd (n,2n) ^{109}Pd	88.04	0.25	0.368	0.11	1	0.7477
46, #2	^{102}Pd (n,2n) ^{101}Pd	296.3	0.008	17.03	2.4	1.167	0.9992
	^{102}Pd (n,np) ^{101m}Rh	306.8				1	0.9993
	^{110}Pd (n,2n) ^{109}Pd	88.04				1	0.9903
	^{105}Pd (n,p) ^{105}Rh	319.1				1	0.9993
	^{108}Pd (n,α) ^{105}Ru	724.2				0.999	0.9997
47, #1	^{107}Ag (n,2n) ^{106m}Ag	450.98	0.1	0.75	0.13	1	0.9947
47, #2	^{107}Ag (n,2n) ^{106m}Ag	450.98	0.1	8.59	2.3	1	0.9947

Table 2 (continued-1)

Z	Reactions	Energy (keV)	Thickness of target (mm)	Neutron flux Total ($x10^{16}$)	Neutron flux Average ($x10^{12}/s$)	Correction factors K	Correction factors μ
48, #2	^{116}Cd (n,2n) ^{115g}Cd	336.24	0.005	16.15	2.2	1	0.9997
	^{112}Cd (n,p) ^{112}Ag	617.3				1	0.9998
48, #1	^{116}Cd (n,2n) ^{115g}Cd	336.24	0.25	0.256	0.11	1	0.9857
49, #2	^{115}In (n,2n) ^{114m}In	190.29	0.01	17.29	2.4	1	0.9989
	(n,α) ^{112}Ag	617.3				1	0.9997
49, #1	^{115}In (n,2n) ^{114m}In	190.29	0.1	0.256	0.11	1	0.9888
73	^{181}Ta (n,2n) ^{180m}Ta	93	0.01	6.33	2.5	1	0.9545
75	^{187}Re (n,2n) ^{186}Re	137.16	0.05	0.748	0.13	1	0.9034
78	^{196}Pt (n,2n) ^{195}Pt	98.9	0.01	14.98	2.1	1.004	0.9485
	^{198}Pt (n,2n) ^{197}Pt	191				1.062	0.9906
79, #2	^{197}Au (n,2n) ^{196g}Au	355.65	0.02	7.99	2.3	1	0.9947
	^{196m}Au	188.23				1	0.9813
79, #1	^{197}Au (n,2n) ^{196g}Au	355.65	0.02	0.877	0.18	1	0.9947
82	^{204}Pb (n,2n) ^{203}Pb	279.2	0.2	19.42	1.8	1.004	0.9521
SS316	^{56}Fe (n,p) ^{56}Mn	846.75	0.1	16.68	2.3	1.037	0.9975
	^{52}Cr (n,2n) ^{51}Cr	320				1	0.9958
	^{58}Ni (n,p) ^{58}Co	811				1	0.9974
	(n,np) ^{57}Co	122				1.036	0.9874
	(n,2n) ^{57}Ni	1377.6				1	0.9979

*: Targets with 0.025 mm thickness were used at the distances of 0.5 and 1 mm and target with 0.25mm thickness was used at the distance 2 mm.

**: Target with a polyester support.

Table 3 Forward and backward sputtering yields by 14.9 MeV neutrons.

Reactions	σ (barn)	Forward and Backward	Distances between sample and collector foils (mm) 0.2	0.5	1	2	3	5	S_n (1/neutron)	RS_n (1/barn)	F/B
$^{19}F(n,2n)^{18}F$	0.0518	Forward	-	5.95E-07	4.21E-07	3.97E-07	3.34E-07	-	5.89E-07	1.14E-05	1.5
		Error	-	7.78E-08	5.57E-08	5.14E-08	4.35E-08	-	8.834E-08	1.71E-06	
		Backward	-	-	3.72E-07	3.62E-07	3.23E-07	-	4.05E-07	7.82E-06	
		Error	-	-	4.83E-08	4.71E-08	4.25E-08	-	6.077E-08	1.17E-06	
$^{24}Mg(n,p)^{24}Na$	0.168	Forward	-	9.14E-07	6.09E-07	3.38E-07	2.29E-07	1.34E-07	9.46E-07	5.63E-06	173
		Error	-	1.16E-07	7.77E-08	4.33E-08	3.73E-08	2.32E-08	1.11E-07	6.61E-07	
		Backward	-	4.71E-09	1.92E-09	1.42E-09	-	-	5.47E-09	3.26E-08	
		Error	-	6.66E-10	2.94E-10	2.47E-10	-	-	7.00E-10	4.17E-09	
$^{27}Al(n,\alpha)^{24}Na$	0.1139	Forward	6.10E-07	5.69E-07	5.05E-07	3.94E-07	2.98E-07	1.61E-07	6.62E-07	5.81E-06	20
		Error	7.81E-08	7.28E-08	6.45E-08	5.04E-08	4.07E-08	2.38E-08	8.59E-08	7.54E-07	
		Backward	3.12E-08	2.04E-08	1.40E-08	7.21E-09	-	-	3.27E-08	2.87E-07	
		Error	4.26E-09	2.73E-09	1.90E-09	9.92E-10	-	-	4.80E-09	4.21E-08	
$^{27}Al(n,p)^{27}Mg$	0.0623	Forward 1	-	2.37E-07	1.96E-07	1.28E-07	8.58E-08	4.25E-08	2.82E-07	4.53E-06	83
		Error	-	3.02E-08	2.51E-08	1.64E-08	1.20E-08	5.50E-09	3.67E-08	5.89E-07	
		Forward 2	-	2.33E-07	2.01E-07	1.24E-07	5.70E-08	4.78E-08	2.63E-07	4.22E-06	
		Error	-	3.00E-08	2.62E-08	1.62E-08	7.89E-09	6.38E-09	3.46E-08	5.55E-07	
		Backward	-	1.21E-09	4.27E-10	-	-	-	3.42E-09	5.49E-08	
		Error	-	2.25E-10	1.41E-10	-	-	-	6.80E-10	1.09E-08	
$^{45}Sc(n,\alpha)^{42}K$	0.0533	Forward	-	7.92E-08	6.99E-08	4.84E-08	-	-	9.52E-08	1.79E-06	5
		Error	-	1.03E-08	9.03E-09	6.31E-09	-	-	1.24E-08	2.33E-07	
		Backward	-	1.08E-08	6.06E-09	-	-	-	1.92E-08	3.6E-07	
		Error	-	1.52E-09	8.47E-10	-	-	-	3.00E-09	5.63E-08	
$^{45}Sc(n,2n)^{44m}Sc$	0.131	Forward	-	5.74E-08	3.78E-08	1.98E-08	-	-	7.93E-08	6.05E-07	
		Error	-	7.38E-09	4.88E-09	2.55E-09	-	-	1.14E-08	8.7E-08	
$^{48}Ti(n,p)^{48}Sc$	0.0596	Forward 1	-	3.94E-08	1.98E-08	1.04E-08	6.47E-09	-	4.67E-08	7.83E-07	
		Error	-	5.14E-09	2.62E-09	1.38E-09	8.37E-10	-	6.08E-09	1.02E-07	
		Forward 2	-	4.19E-08	2.01E-08	1.21E-08	7.04E-09	-	4.84E-08	8.11E-07	
		Error	-	5.50E-09	2.66E-09	1.60E-09	9.09E-10	-	7.50E-09	1.26E-07	
$^{48}Ti(n,np)^{47}Sc$	0.0207	Forward	-	1.47E-08	7.39E-09	3.95E-09	2.64E-09	-	1.70E-08	8.21E-07	
		Error	-	1.96E-09	1.02E-09	5.67E-10	3.61E-10	-	2.50E-09	1.21E-07	
$^{51}V(n,\alpha)^{48}Sc$	0.0169	Forward 1	-	1.82E-08	1.68E-08	8.84E-09	5.82E-09	3.11E-09	2.15E-08	1.27E-06	11
		Error	-	2.40E-09	2.24E-09	1.16E-09	8.15E-10	4.42E-10	2.79E-09	1.65E-07	
		Forward 2	-	1.68E-08	1.57E-08	8.76E-09	6.30E-09	3.16E-09	2.07E-08	1.23E-06	
		Error	-	2.25E-09	2.12E-09	1.15E-09	8.72E-10	4.51E-10	2.58E-09	1.53E-07	
		Backward	-	1.28E-09	4.60E-10	2.10E-10	-	-	1.89E-09	1.12E-07	
		Error	-	2.50E-10	1.10E-10	6.60E-11	-	-	3.00E-10	1.78E-08	
$^{52}Cr(n,2n)^{51}Cr$	0.376	Forward	-	1.85E-07	9.10E-08	5.02E-08	3.13E-08	-	2.15E-07	5.71E-07	
		Error	-	2.54E-08	1.43E-08	6.62E-09	4.22E-09	-	3.00E-08	7.98E-08	
SS316 $^{52}Cr(n,2n)^{51}Cr$	0.376	Forward	-	9.17E-08	6.31E-08	2.92E-08	1.24E-08	-	1.39E-07	3.71E-07	
		Error	-	1.46E-08	9.52E-09	3.79E-09	6.83E-09	-	2.37E-08	6.3E-08	

Table 3 (continued-1)

Reactions	σ (barn)	Forward and Backward	Distances between sample and collector foils (mm) 0.2	0.5	1	2	3	5	S_n (1/neutron)	RS_n (1/barn)	F/B
^{56}Fe(n,p)^{56}Mn	0.111	Forward	5.62E-08	4.51E-08	2.28E-08	1.18E-08	7.54E-09	-	5.84E-08	5.26E-07	96
		Error	7.23E-09	5.79E-09	2.95E-09	1.53E-09	9.87E-10	-	7.60E-09	6.84E-08	
		Backward	3.30E-10	1.30E-10	-	-	-	-	6.11E-10	5.51E-09	
		Error	9.24E-11	4.45E-11	-	-	-	-	1.90E-10	1.71E-09	
SS316 ^{56}Fe(n,p)^{56}Mn	0.111	Forward	-	2.67E-08	1.53E-08	7.71E-09	-	-	3.79E-08	3.42E-07	104
		Error	-	3.40E-09	1.96E-09	9.94E-10	-	-	5.69E-09	5.13E-08	
		Backward	-	2.21E-10	2.71E-10	1.00E-10	-	-	3.64E-10	3.27E-09	
		Error	-	3.73E-11	4.96E-11	2.30E-11	-	-	7.27E-11	6.55E-10	
^{59}Co(n,α)^{56}Mn	0.0323	Forward	-	3.09E-08	2.39E-08	1.39E-08	1.03E-08	4.65E-09	3.57E-08	1.11E-06	19
		Error	-	3.94E-09	3.08E-09	1.80E-09	1.37E-09	6.47E-10	4.65E-09	1.44E-07	
		Backward	-	1.35E-09	8.64E-10	4.24E-10	-	-	1.92E-09	5.94E-08	
		Error	-	1.89E-10	1.17E-10	6.90E-11	-	-	2.50E-10	7.74E-09	
^{59}Co(n,2n)^{58}Co	0.63	Forward	-	1.25E-07	6.99E-08	3.53E-08	2.78E-08	-	1.41E-07	2.25E-07	
		Error	-	1.60E-08	9.20E-09	4.81E-09	4.50E-09	-	1.88E-08	2.98E-08	
^{59}Co(n,p)^{59}Fe	0.0457	Forward	-	1.29E-08	9.43E-09	-	-	-	1.77E-08	3.88E-07	
		Error	-	2.21E-09	2.40E-09	-	-	-	2.70E-09	5.91E-08	
^{58}Ni(n,p)^{58}Co	0.269	Forward	-	7.00E-08	5.44E-08	2.63E-08	2.07E-08	-	8.72E-08	3.24E-07	
		Error	-	1.00E-08	7.01E-09	3.69E-09	2.95E-09	-	1.25E-08	4.65E-08	
SS316 ^{58}Ni(n,p)^{58}Co	0.269	Forward	-	6.81E-08	4.21E-08	1.82E-08	-	-	1.04E-07	3.85E-07	
		Error	-	1.03E-08	6.37E-09	3.36E-09	-	-	1.66E-08	6.17E-08	
^{58}Ni(n,2n)^{57}Ni	0.042	Forward	-	9.05E-09	5.15E-09	2.86E-09	2.88E-09	-	9.17E-09	2.18E-07	
		Error	-	1.20E-09	6.61E-10	4.02E-10	4.57E-10	-	1.25E-09	2.98E-08	
SS316 ^{58}Ni(n,2n)^{57}Ni	0.042	Forward	-	6.43E-09	3.90E-09	2.31E-09	-	-	8.36E-09	1.99E-07	
		Error	-	9.03E-10	5.86E-10	4.13E-10	-	-	1.25E-09	2.99E-08	
^{58}Ni(n,np)^{57}Co	0.661	Forward	-	2.11E-07	1.33E-07	5.91E-08	4.17E-08	-	2.64E-07	3.99E-07	
		Error	-	2.80E-08	1.70E-08	8.16E-09	6.14E-09	-	3.48E-08	5.26E-08	
SS316 ^{58}Ni(n,np)^{57}Co	0.661	Forward	-	1.53E-07	9.80E-08	5.35E-08	-	-	2.07E-07	3.14E-07	
		Error	-	2.93E-08	1.56E-08	1.18E-08	-	-	4.15E-08	6.27E-08	
^{65}Cu(n,p)^{65}Ni	0.0188	Forward	-	3.18E-09	2.09E-09	-	-	-	4.84E-09	2.58E-07	
		Error	-	6.99E-10	6.20E-10	-	-	-	9.50E-10	5.05E-08	
^{65}Cu(n,2n)^{64}Cu	0.961	Forward	-	1.55E-07	7.89E-08	3.31E-08	2.74E-08	-	1.77E-07	1.84E-07	29
		Error	-	1.99E-08	1.02E-08	4.35E-09	3.58E-09	-	2.50E-08	2.6E-08	
		Backward	-	4.92E-09	4.72E-09	3.07E-09	-	-	6.10E-09	6.35E-09	
		Error	-	8.03E-10	6.98E-10	4.69E-10	-	-	1.10E-09	1.14E-09	
^{90}Zr(n,2n)^{89}Zr	0.832	Forward	5.25E-08	3.51E-08	1.63E-08	8.03E-09	-	-	5.78E-08	6.94E-08	57
		Error	6.92E-09	4.65E-09	2.10E-09	1.09E-09	-	-	7.54E-09	9.06E-09	
		Backward	9.79E-10	1.03E-09	1.02E-09	-	-	-	1.02E-09	1.22E-09	
		Error	2.79E-10	2.62E-10	1.74E-10	-	-	-	2.80E-10	3.37E-10	
^{90}Zr(n,p)^{90m}Y	0.0124	Forward	1.07E-09	7.32E-10	-	-	-	-	1.37E-09	1.11E-07	
		Error	2.37E-10	1.34E-10	-	-	-	-	2.80E-10	2.26E-08	

Table 3 (continued-2)

Reactions	σ (barn)	Forward and Backward	Distances between sample and collector foils (mm) 0.2	0.5	1	2	3	5	S_n (1/neutron)	RS_n (1/barn)	F/B
^{90}Zr(n,α)^{87m}Sr	0.0038	Forward	7.59E-10	5.31E-10	-	-	-	-	9.21E-10	2.41E-07	
		Error	1.99E-10	1.23E-10	-	-	-	-	2.40E-10	6.28E-08	
^{93}Nb(n,2n)^{92m}Nb #1 sample	0.464	Forward	2.32E-08	1.68E-08	7.53E-09	3.62E-09	-	-	2.66E-08	5.73E-08	
		Error	3.15E-09	2.15E-09	1.02E-09	5.29E-10	-	-	3.75E-09	8.08E-09	
^{93}Nb(n,2n)^{92m}Nb #2 sample	0.464	Forward	-	1.46E-08	7.01E-09	3.44E-09	-	-	2.08E-08	4.48E-08	
		Error	-	1.89E-09	9.26E-10	4.78E-10	-	-	3.00E-09	6.47E-09	
^{93}Nb(n,α)^{90m}Y #1 sample	0.0049	Forward	8.45E-10	6.79E-10	-	-	-	-	9.78E-10	1.98E-07	
		Error	1.29E-10	9.88E-11	-	-	-	-	1.50E-10	3.04E-08	
^{93}Nb(n,α)^{90m}Y #2 sample	0.0049	Forward	-	8.69E-10	5.67E-10	2.41E-10	-	-	1.33E-09	2.70E-07	
		Error	-	1.16E-10	7.66E-11	3.69E-11	-	-	2.00E-10	4.05E-08	
^{100}Mo(n,2n)^{99}Mo	1.38	Forward	-	2.19E-08	7.99E-09	-	-	-	6.01E-08	4.35E-08	
		Error	-	3.81E-09	1.51E-09	-	-	-	1.14E-08	8.27E-09	
^{92}Mo(n,a)^{89}Zr	0.0256	Forward	-	4.81E-09	2.79E-09	1.73E-09	1.52E-09	-	4.99E-09	1.95E-07	
		Error	-	6.46E-10	3.80E-10	2.63E-10	2.76E-10	-	7.49E-10	2.93E-08	
^{92}Mo(n,p)^{92m}Nb	0.0588	Forward	-	1.75E-09	6.83E-10	-	-	-	4.43E-09	7.54E-08	
		Error	-	3.49E-10	1.56E-10	-	-	-	1.02E-09	1.73E-08	
^{96}Mo(n,p)^{96}Nb	0.0247	Forward	-	3.81E-10	7.23E-11	-	-	-	2.01E-09	8.13E-08	
		Error	-	1.31E-10	2.97E-11	-	-	-	8.03E-10	3.25E-08	
^{110}Pd(n,2n)^{109}Pd #1 sample	1.55	Forward	-	2.64E-08	1.16E-08	-	-	-	6.01E-08	3.88E-08	
		Error	-	7.65E-09	5.64E-09	-	-	-	1.76E-08	1.14E-08	
^{110}Pd(n,2n)^{109}Pd #2 sample	1.55	Forward	-	4.61E-08	2.40E-08	1.37E-08	-	-	5.96E-08	3.85E-08	
		Error	-	6.23E-09	3.26E-09	1.90E-09	-	-	8.94E-09	5.77E-09	
^{102}Pd(n,2n)^{101}Pd #2 sample	1.179	Forward	-	2.71E-08	2.15E-08	7.48E-08	-	-	4.59E-08	3.9E-08	
		Error	-	4.64E-09	3.84E-09	3.00E-09	-	-	9.19E-09	7.79E-09	
^{108}Pd(n,a)^{105}Ru #2 sample	0.0033	Forward	-	1.60E-10	3.91E-11	-	-	-	6.55E-10	1.97E-07	
		Error	-	3.68E-11	1.76E-11	-	-	-	1.96E-10	5.9E-08	
^{105}Pd(n,p)^{105}Rh #2 sample	0.0427	Forward	-	1.44E-09	6.81E-10	-	-	-	3.04E-09	7.13E-08	
		Error	-	2.84E-10	2.05E-10	-	-	-	6.09E-10	1.43E-08	
^{102}Pd(n,np)^{101m}Rh #2 sample	0.27	Forward	-	5.81E-09	3.61E-09	7.88E-10	-	-	1.24E-08	4.61E-08	
		Error	-	9.32E-10	6.26E-10	3.54E-10	-	-	2.49E-09	9.21E-09	
^{107}Ag(n,2n)^{106m}Ag #1 sample	0.557	Forward	-	1.16E-08	6.45E-09	-	-	-	1.97E-08	3.54E-08	
		Error	-	3.50E-09	1.64E-09	-	-	-	6.3E-09	1.13E-08	
^{107}Ag(n,2n)^{106m}Ag #2 sample	0.557	Forward	-	1.10E-08	4.94E-09	2.46E-09	-	-	1.56E-08	2.81E-08	
		Error	-	1.51E-09	7.04E-10	5.36E-10	-	-	2.503E-09	4.49E-09	
^{116}Cd(n,2n)^{115g}Cd #1 sample	0.78	Forward	-	8.90E-09	4.11E-09	-	-	-	1.93E-08	2.47E-08	
		Error	-	2.74E-09	1.49E-09	-	-	-	6.00E-09	7.69E-09	
^{116}Cd(n,2n)^{115g}Cd #2 sample	0.78	Forward	-	1.60E-08	9.14E-09	6.16E-09	-	-	1.95E-08	2.5E-08	
		Error	-	2.12E-09	1.26E-09	9.64E-10	-	-	3.00E-09	3.85E-09	
^{112}Cd(n,p)^{112}Ag #2 sample	0.0181	Forward	-	3.48E-10	1.40E-10	-	-	-	8.65E-10	4.78E-08	
		Error	-	9.49E-11	7.65E-11	-	-	-	2.50E-10	1.38E-08	

Table 3 (continued-3)

Reactions	σ (barn)	Forward and Backward	Distances between sample and collector foils (mm) 0.2	0.5	1	2	3	5	S_n (1/neutron)	RS_n (1/barn)	F/B
^{115}In(n,2n)^{114}In	1.255	Forward	-	1.21E-08	4.57E-09	-	-	-	3.21E-08	2.56E-08	
#1 sample		Error	-	3.08E-09	1.32E-09	-	-	-	7.70E-09	6.14E-09	
^{115}In(n,2n)^{114}In	1.255	Forward	-	1.54E-08	7.82E-09	-	-	-	3.04E-08	2.42E-08	
#2 sample		Error	-	2.17E-09	1.42E-09	-	-	-	5.47E-09	4.36E-09	
^{115}In(n,α)^{112}Ag	0.0027	Forward	-	2.00E-10	1.19E-10	-	-	-	3.35E-10	1.26E-07	
#2 sample		Error	-	3.86E-11	3.19E-11	-	-	-	8.38E-11	3.15E-08	
^{181}Ta(n,2n)^{180m}Ta	1.297	Forward	-	5.91E-09	4.40E-09	1.83E-09	1.06E-09	-	8.45E-09	6.52E-09	
		Error	-	8.92E-10	9.24E-10	2.67E-10	3.13E-10	-	1.52E-09	1.17E-09	
^{187}Re(n,2n)^{186}Re	1.56	Forward	-	5.42E-09	3.32E-09	1.43E-09	-	-	8.25E-09	5.29E-09	
		Error	-	1.38E-09	5.89E-10	3.31E-10	-	-	2.27E-09	1.46E-09	
^{196}Pt(n,2n)^{195}Pt	1.692	Forward	-	6.43E-09	4.17E-09	1.70E-09	-	-	1.01E-08	5.96E-09	
		Error	-	1.14E-09	7.38E-10	4.81E-10	-	-	1.50E-09	8.87E-10	
^{198}Pt(n,2n)^{197}Pt	1.1	Forward	-	3.99E-09	2.46E-09	-	-	-	6.47E-09	5.88E-09	
		Error	-	1.05E-09	6.89E-10	-	-	-	1.50E-09	1.36E-09	
^{197}Au(n,2n)^{196g}Au	1.894	Forward	-	8.38E-09	5.73E-09	2.31E-09	1.17E-09	-	1.24E-08	6.55E-09	113
		Error	-	1.09E-09	7.80E-10	3.34E-10	1.81E-10	-	1.62E-09	8.55E-10	
#1 sample		Backward	-	1.05E-10	1.12E-10	-	-	-	1.10E-10	5.81E-11	
		Error	-	4.39E-11	3.29E-11	-	-	-	4.50E-11	2.38E-11	
^{197}Au(n,2n)^{196g}Au	1.894	Forward	-	6.23E-09	2.75E-09	9.20E-10	-	-	1.08E-08	5.68E-09	29
		Error	-	8.38E-10	3.72E-10	1.31E-10	-	-	1.61E-09	8.53E-10	
#2 sample		Backward	-	2.05E-10	1.12E-10	-	-	-	3.77E-10	1.99E-10	
		Error	-	1.12E-10	2.83E-11	-	-	-	2.07E-10	1.1E-10	
^{197}Au(n,2n)^{196m}Au	1.3	Forward	-	6.07E-09	2.45E-09	1.20E-09	-	-	8.67E-09	6.67E-09	
#2 sample		Error	-	9.72E-10	4.17E-10	2.16E-10	-	-	1.56E-09	1.2E-09	
^{204}Pb(n,2n)^{203}Pb	2.12	Forward	-	4.70E-09	2.09E-09	-	-	-	1.06E-08	5E-09	
		Error	-	1.28E-09	6.06E-10	-	-	-	3.18E-09	1.5E-09	

Table 4 The fitting parameters of the systematics for RS_n

reactions	a	b
(n, p)	0.026312	-3.3846
(n, α)	0.011956	-2.9149
(n, 2n)	0.028811	-3.5487
(n,np)	0.17452	-3.9481

Table 5 The Comparison of present results with others experimental results for RS_n.

Reactions	Cross Section (mb)	Present systematics (1/barn)	Present measurement (1/barn)	Y.Ikeda Ref.23 (1/barn)	M.Thomas Ref.42 (1/barn)	R.Behrisch Ref.43 (1/barn)	O.Harling Ref.4 (1/barn)
$^{24}Mg(n,p)^{24}Na$	167.6	5.86E-06	5.65E-06				
$^{27}Al(n,p)^{27}Mg$	62.3	4.47E-06	4.45E-06				
$^{46}Ti(n,p)^{46}Sc$	270	7.53E-07					9.185E-08
$^{48}Ti(n,p)^{48}Sc$	59.6	7.89E-07	7.83E-07				7.181E-07
$^{56}Fe(n,p)^{56}Mn$	111	4.28E-07	5.26E-07	8.00E-07			1.61E-07
$^{59}Co(n,p)^{59}Fe$	45.7	3.76E-07	3.88E-07				
$^{58}Ni(n,p)^{58}Co$	269	3.33E-07	3.24E-07	8.50E-07	7.40E-08		6.32E-07
$^{60}Ni(n,p)^{60}Co$	130.3	3.33E-07		7.80E-07	2.20E-08		2.14E-07
$^{65}Cu(n,p)^{65}Ni$	18.8	3.02E-07	2.58E-07				
$^{90}Zr(n,p)^{90m}Y$	12.38	9.95E-08	1.10E-07				
$^{92}Mo(n,p)^{92m}Nb$	58.8	8.44E-08	7.54E-08		4.05E-08		
$^{95}Mo(n,p)^{95}Nb$	41.9	8.44E-08		2.00E-07	3.82E-08		
$^{95}Mo(n,p)^{95m}Nb$	60	8.44E-08			3.87E-09		
$^{96}Mo(n,p)^{96}Nb$	24.7	8.44E-08	8.13E-08		3.32E-07		
$^{105}Pd(n,p)^{105}Rh$, #2	42.7	6.2E-08	7.13E-08				
$^{112}Cd(n,p)^{112}Ag$, #2	18.1	5.37E-08	4.78E-08				
$SS316(n,p)^{56}Mn$	111	4.28E-07	3.42E-07				
$SS316(n,p)^{58}Co$	269	3.33E-07	3.85E-07		7.40E-08		
$^{27}Al(n,\alpha)^{24}Na$	113.9	6.77E-06	5.81E-06	7.00E-06			
$^{45}Sc(n,\alpha)^{42}K$	53.3	1.67E-06	1.79E-06				
$^{50}Ti(n,\alpha)^{47}Ca$	10	1.46E-06					1.01E-07
$^{50}V(n,\alpha)^{47}Sc$	50	1.28E-06					4.32E-09
$^{51}V(n,\alpha)^{48}Sc$	16.9	1.28E-06	1.27E-06	2.00E-06			1.56E-06
$^{54}Fe(n,\alpha)^{51}Cr$	96	8.98E-07					1.24E-07
$^{59}Co(n,\alpha)^{56}Mn$	32.3	8.04E-07	1.11E-06				
$^{63}Cu(n,\alpha)^{60}Co$	45	6.53E-07					9.33E-07
$^{62}Ni(n,\alpha)^{59}Fe$	24	7.23E-07					4.63E-08
$^{90}Zr(n,\alpha)^{87m}Sr$	3.82	2.56E-07	2.41E-07				
$^{93}Nb(n,\alpha)^{90m}Y$, #1	4.94	2.38E-07	1.98E-07	8.00E-07			
$^{93}Nb(n,\alpha)^{90m}Y$, #2	4.94	2.38E-07	2.70E-07				
$^{92}Mo(n,\alpha)^{89m+g}Zr$	25.6	2.22E-07	1.95E-07				
$^{108}Pd(n,\alpha)^{105}Ru$, #2	3.33	1.7E-07	1.97E-07				
$^{115}In(n,\alpha)^{112}Ag$, #2	2.66	1.42E-07	1.26E-07				

Table 5 (continued-1)

Reactions	Cross Section (mb)	Present systematics (1/barn)	Present measurement (1/barn)	Y.Ikeda Ref.23 (1/barn)	M.Thomas Ref.42 (1/barn)	R.Behrisch Ref.43 (1/barn)	O.Harling Ref.4 (1/barn)
^{19}F(n,2n)^{18}F	51.8	1.11E-05	1.14E-05				
^{45}Sc(n, 2n)^{44m}Sc	131	5.84E-07	6.05E-07				
^{52}Cr(n,2n)^{51}Cr	376	3.64E-07	5.71E-07	1.00E-06			8.43E-07
^{59}Co(n,2n)^{58}Co	630	2.4E-07	2.25E-07				
^{58}Ni(n,2n)^{57}Ni	42	2.11E-07	2.18E-07	4.00E-07	7.42E-08		
^{65}Cu(n,2n)^{64}Cu	961	1.84E-07	1.84E-07				
^{90}Zr(n,2n)^{89}Zr	832	5.97E-08	6.94E-08				
^{93}Nb(n,2n)^{92m}Nb, #1	464	5.47E-08	5.73E-08	2.50E-07	2.28E-07	1.70E-07	1.58E-07
^{93}Nb(n,2n)^{92m}Nb, #2	464	5.47E-08	4.48E-08				
^{100}Mo(n,2n)^{99}Mo	1380	5.03E-08	4.35E-08	2.50E-07	2.07E-08		
^{110}Pd(n,2n)^{109}Pd, #1	1550	3.64E-08	3.88E-08				
^{110}Pd(n,2n)^{109}Pd, #2	1550	3.64E-08	3.85E-08				
^{102}Pd(n,2n)^{101}Pd, #2	1179	3.64E-08	3.89E-08				
^{107}Ag(n,2n)^{106m}Ag, #1	557	3.38E-08	3.54E-08				
^{107}Ag(n,2n)^{106m}Ag, #2	557	3.38E-08	2.81E-08				
^{116}Cd(n,2n)^{115g}Cd, #1	780	3.13E-08	2.47E-08				
^{116}Cd(n,2n)^{115g}Cd, #2	780	3.13E-08	2.50E-08				
^{115}In(n,2n)^{114}In, #1	1255	2.91E-08	2.56E-08				
^{115}In(n,2n)^{114}In, #2	1255	2.91E-08	2.42E-08				
^{181}Ta(n,2n)^{180m}Ta	1297	7.11E-09	6.52E-09				
^{187}Re(n,2n)^{186}Re	1560	6.46E-09	5.29E-09				
^{196}Pt(n,2n)^{195}Pt	1692	5.62E-09	5.97E-09				
^{198}Pt(n,2n)^{197}Pt	1100	5.62E-09	5.88E-09				
^{197}Au(n,2n)^{196}Au, #1	1894	5.37E-09	6.53E-09	6.00E-08		5.81E-08	5.50E-08
^{197}Au(n,2n)^{196}Au, #2	1894	5.37E-09	5.68E-09				
^{197}Au(n,2n)^{196m}Au, #2	1300	5.37E-09	6.67E-09				
^{204}Pb(n,2n)^{203}Pb	2120	4.71E-09	5.01E-09				
SS316(n,2n)^{51}Cr	376	3.64E-07	3.71E-07		2.15E-07		
SS316(n,2n)^{57}Ni	42	2.11E-07	1.99E-07		7.38E-08		
^{48}Ti(n,np)^{47}Sc	20.7	8.75E-07	8.21E-07				
^{58}Ni(n,np)^{57}Co	661	3.38E-07	3.99E-07				
SS316(n,np)^{57}Co	661	3.38E-07	3.14E-07		7.56E-08		
^{102}Pd(n,np)^{101m}Rh, #2	270	4.75E-08	4.61E-08				

Table 6 The results of the theoretical calculation for the neutron sputtering yield

Reactions	A1	A2	Z1	Z2	σ	T	ρ	<R>	$S_{n,f}$	$RS_{n,f}$(1/barn)		C/E
					(mb)	(KeV)	(g/cm^3)	(cm)	(1/neutron)	Calculation	Experiment	
^{24}Mg(n,p)^{24}Na	24	24	12	11	168	572	1.74	0.000118	8.66E-07	5.17E-06	5.63E-06	0.92
^{27}Al(n,p)^{27}Mg	27	27	13	12	62.3	513	2.7	6.69E-05	2.51E-07	4.03E-06	4.53E-06	0.89
^{48}Ti(n,p)^{48}Sc	48	48	22	21	60.4	298	4.5	1.68E-05	5.72E-08	9.47E-07	7.83E-07	1.21
^{56}Fe(n,p)^{56}Mn	56	56	26	25	111	257	7.8	7.32E-06	6.82E-08	6.14E-07	5.26E-07	1.17
^{59}Co(n,p)^{59}Fe	59	59	27	26	45.7	244	8.83	6.08E-06	2.5E-08	5.48E-07	3.88E-07	1.41
^{58}Ni(n,p)^{58}Co	58	58	28	27	269	248	8.85	5.7E-06	1.41E-07	5.23E-07	3.24E-07	1.62
^{65}Cu(n,p)^{65}Ni	65	65	29	28	18.8	222	8.93	5.34E-06	8.3E-09	4.42E-07	2.57E-07	1.72
^{90}Zr(n,p)^{90m}Y	90	90	40	39	12.4	162	6.52	4.28E-06	2.31E-09	1.87E-07	1.10E-07	1.7
^{92}Mo(n,p)^{92m}Nb	92	92	42	41	58.8	158	10.23	2.51E-06	9.89E-09	1.68E-07	7.53E-08	2.23
^{96}Mo(n,p)^{96}Nb	96	96	42	41	24.7	152	10.23	2.51E-06	3.99E-09	1.61E-07	8.13E-08	1.99
^{105}Pd(n,p)^{105}Rh	105	105	46	45	42.7	139	12.03	1.84E-06	5.41E-09	1.27E-07	7.13E-08	1.78
^{112}Cd(n,p)^{112}Ag	112	112	48	47	18.1	131	8.64	2.38E-06	2.01E-09	1.11E-07	4.78E-08	2.32
^{27}Al(n,a)^{24}Na	27	24	13	11	114	572	2.7	7.14E-05	4.9E-07	4.3E-06	5.81E-06	0.74
^{45}Sc(n,a)^{42}K	45	42	21	19	53.3	338	2.99	2.84E-05	6.05E-08	1.13E-06	1.79E-06	0.63
^{51}V(n,a)^{48}Sc	51	48	23	21	16.9	298	5.98	1.22E-05	1.45E-08	8.59E-07	1.27E-06	0.68
^{59}Co(n,a)^{56}Mn	59	56	27	25	32.3	257	8.83	6.27E-06	1.82E-08	5.65E-07	1.11E-06	0.51
^{90}Zr(n,a)^{87m}Sr	90	87	40	38	3.85	167	6.52	4.37E-06	7.34E-10	1.91E-07	2.41E-07	0.79
^{93}Nb(n,a)^{90m}Y	93	90	41	39	4.94	162	8.56	3.19E-06	8.74E-10	1.77E-07	1.98E-07	0.89
^{92}Mo(n,a)$^{89m+g}$Zr	92	89	42	40	25.6	164	10.23	2.56E-06	4.39E-09	1.72E-07	1.95E-07	0.88
^{108}Pd(n,a)^{105}Ru	108	105	46	44	3.33	139	12.03	1.87E-06	4.18E-10	1.26E-07	1.97E-07	0.64
^{115}In(n,a)^{112}Ag	115	112	49	47	2.66	131	7.28	2.78E-06	2.82E-10	1.06E-07	1.26E-07	0.84
^{19}F(n,2n)^{18}F	19	18	9	9	51.8	743	1.54	0.000196	4.94E-07	9.54E-06	1.14E-05	0.84
^{45}Sc(n,2n)^{44m}Sc	45	44	21	21	130	324	2.99	2.61E-05	1.36E-07	1.05E-06	6.05E-07	1.73
^{52}Cr(n,2n)^{51}Cr	52	51	24	24	376	281	7.19	8.75E-06	2.74E-07	7.29E-07	5.71E-07	1.28
^{59}Co(n,2n)^{58}Co	59	58	27	27	630	248	8.83	5.88E-06	3.34E-07	5.3E-07	2.25E-07	2.36
^{58}Ni(n,2n)^{57}Ni	58	57	28	28	42	252	8.85	5.52E-06	2.13E-08	5.07E-07	2.18E-07	2.33
^{65}Cu(n,2n)^{64}Cu	65	64	29	29	961	226	8.92	5.19E-06	4.12E-07	4.29E-07	1.84E-07	2.33
^{90}Zr(n,2n)^{89}Zr	90	89	40	40	832	164	6.52	4.19E-06	1.52E-07	1.83E-07	6.94E-08	2.63
^{93}Nb(n,2n)^{92m}Nb	93	92	41	41	464	158	8.56	3.06E-06	7.88E-08	1.7E-07	5.73E-08	2.96
^{100}Mo(n,2n)^{99}Mo	100	99	42	42	1380	148	10.23	2.47E-06	2.1E-07	1.52E-07	4.35E-08	3.49
^{110}Pd(n,2n)^{109}Pd	110	109	46	46	1550	134	12.03	1.81E-06	1.84E-07	1.19E-07	3.88E-08	3.06
^{102}Pd(n,2n)^{101}Pd	102	101	46	46	1179	145	12.03	1.8E-06	1.51E-07	1.28E-07	3.90E-08	3.28
^{107}Ag(n,2n)^{106m}Ag	107	106	47	47	557	138	10.49	2E-06	6.57E-08	1.18E-07	3.54E-08	3.33
^{116}Cd(n,2n)^{115g}Cd	116	115	48	48	780	127	8.64	2.34E-06	8.2E-08	1.05E-07	2.47E-08	4.26
^{115}In(n,2n)^{114}In	115	114	49	49	1255	128	7.28	2.69E-06	1.29E-07	1.02E-07	2.56E-08	4
^{181}Ta(n,2n)^{180m}Ta	181	180	73	73	1297	81.9	16.6	6.1E-07	4.37E-08	3.37E-08	6.52E-09	5.17
^{187}Re(n,2n)^{186}Re	187	186	75	75	1560	79.3	21.3	4.55E-07	4.87E-08	3.12E-08	5.29E-09	5.9
^{196}Pt(n,2n)^{195}Pt	196	195	78	78	1692	75.6	21.45	4.23E-07	4.72E-08	2.79E-08	5.97E-09	4.67
^{198}Pt(n,2n)^{197}Pt	198	197	78	78	1100	74.9	21.45	4.23E-07	3.04E-08	2.76E-08	5.88E-09	4.7
^{197}Au(n,2n)^{196g}Au	197	196	79	79	1894	75.3	19.3	4.61E-07	5.15E-08	2.72E-08	6.53E-09	4.16
^{204}Pb(n,2n)^{203}Pb	204	203	82	82	2120	72.7	11.34	7.37E-07	5.23E-08	2.47E-08	5.01E-09	4.93
^{48}Ti(n,np)^{47}Sc	48	47	22	22	20.7	304	4.5	1.61E-05	1.88E-08	9.1E-07	8.21E-07	1.11
^{58}Ni(n,np)^{57}Co	58	57	28	27	661	252	8.85	5.69E-06	3.46E-07	5.23E-07	3.99E-07	1.31
^{102}Pd(n,np)^{101m}Rh	102	101	46	46	270	145	12.03	1.8E-06	3.46E-08	1.28E-07	4.61E-08	2.78

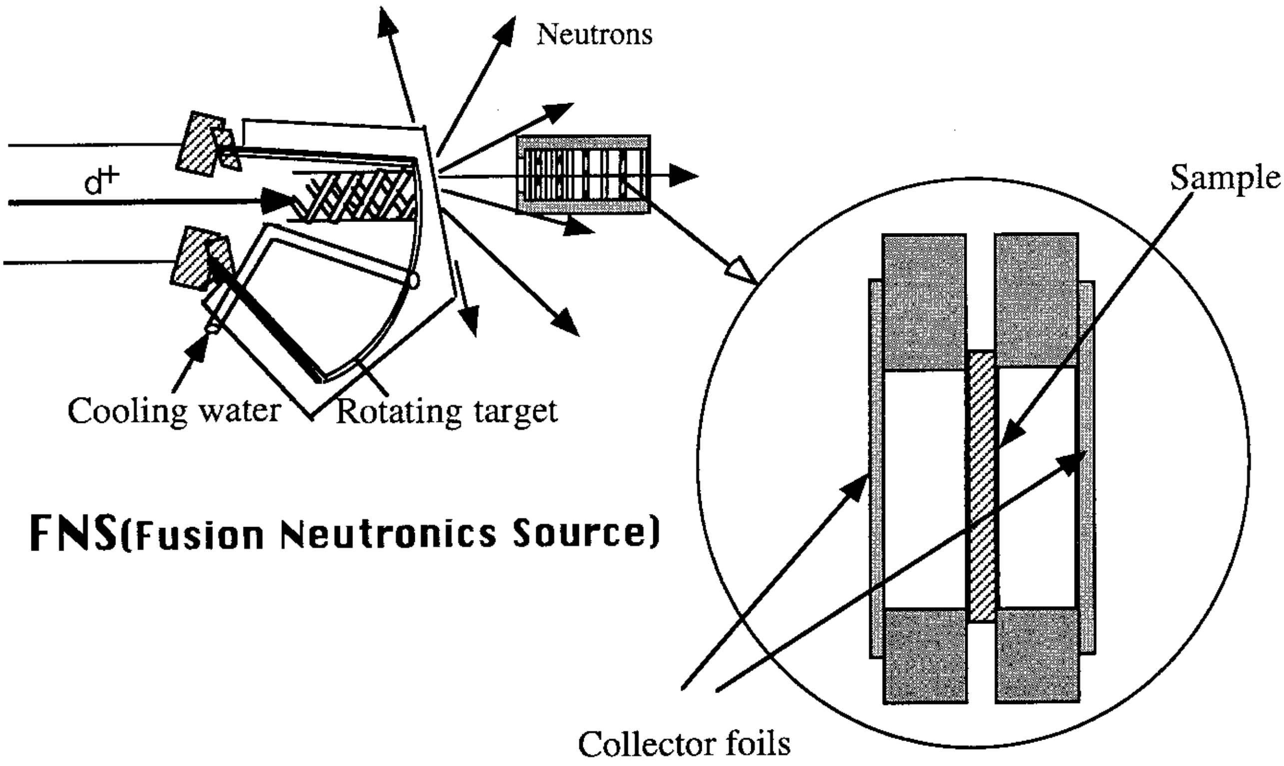

Fig.1 Irradiation configuration of neutron sputtering yields measurement.

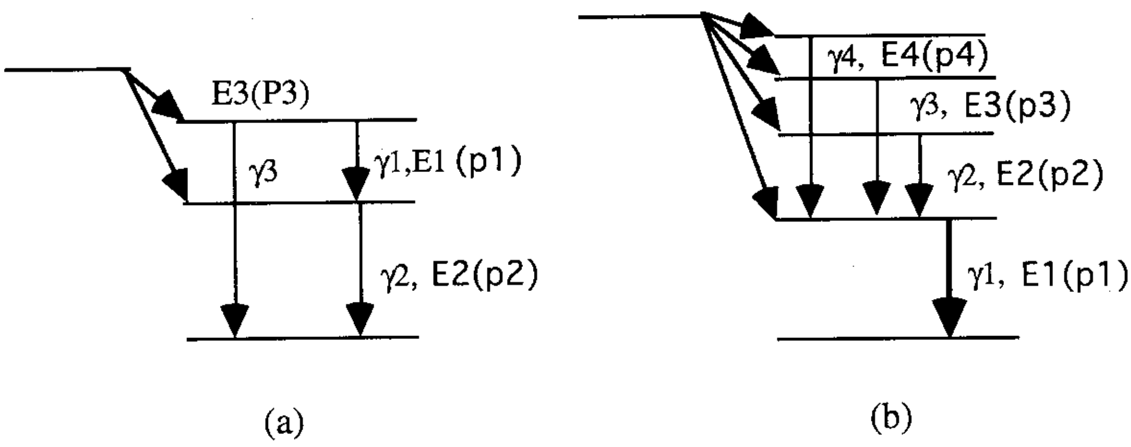

Fig.2 The decay scheme to illustrate the requirement for coincidence- summing corrections. (a) A simple decay scheme, and (b) a complex decay scheme.

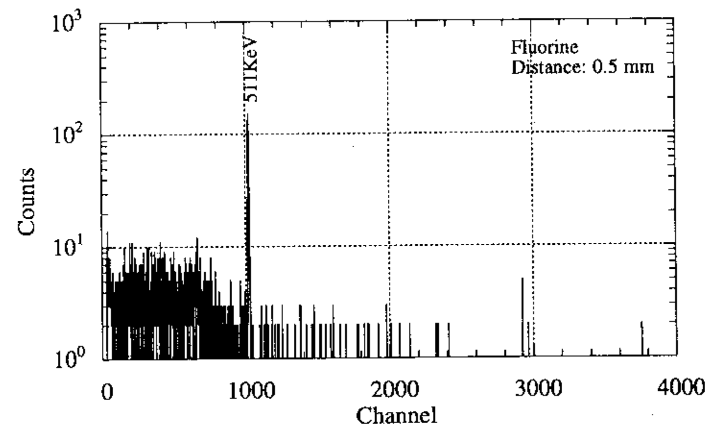

Fig.3 Gamma-ray spectrum of radioactivities emitted from fluorine target irradiated with 14.9 MeV neutrons.

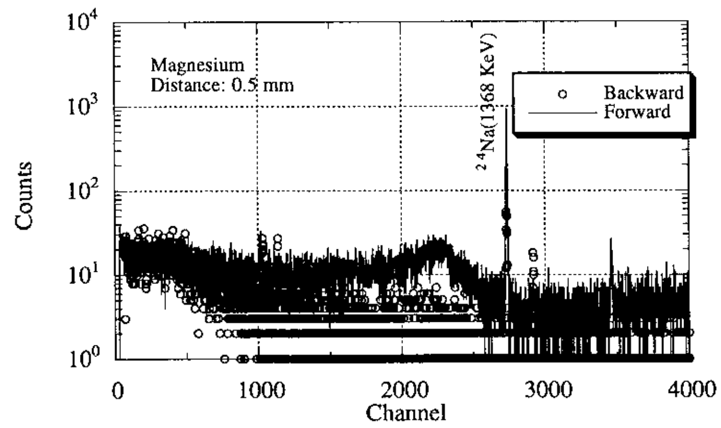

Fig.4 Gamma-ray spectra of radioactivities emitted from magnesium target irradiated by 14.9 MeV neutrons.

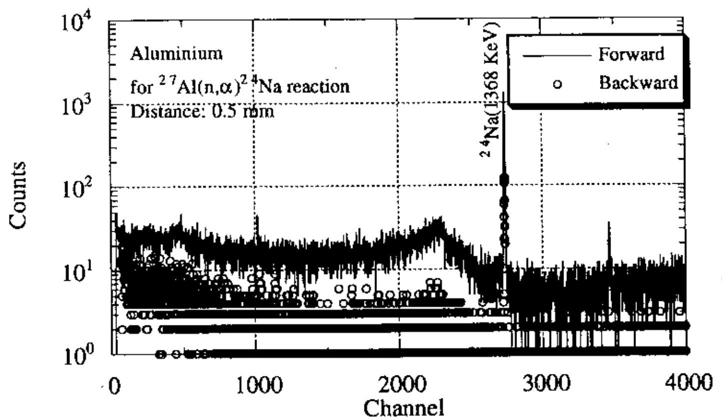

Fig.5 Gamma-ray spectra of radioactivities emitted from aluminium target for (n, α) reaction irradiated with 14.9 MeV neutrons.

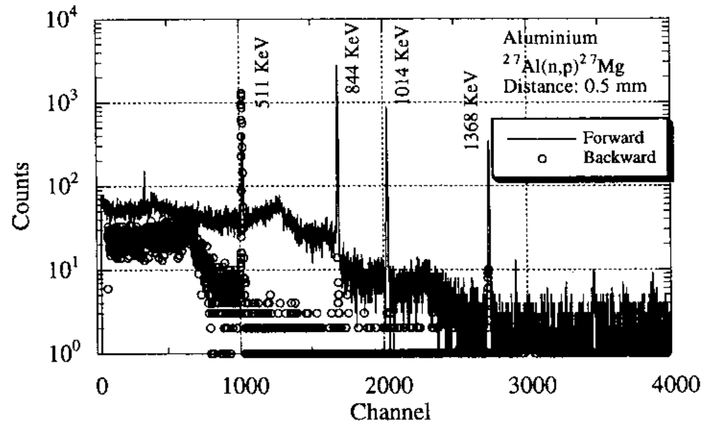

Fig.6 Gamma-ray spectra of radioactivities emitted from aluminium target for (n,p) reaction irradiated with 14.9 MeV neutrons.

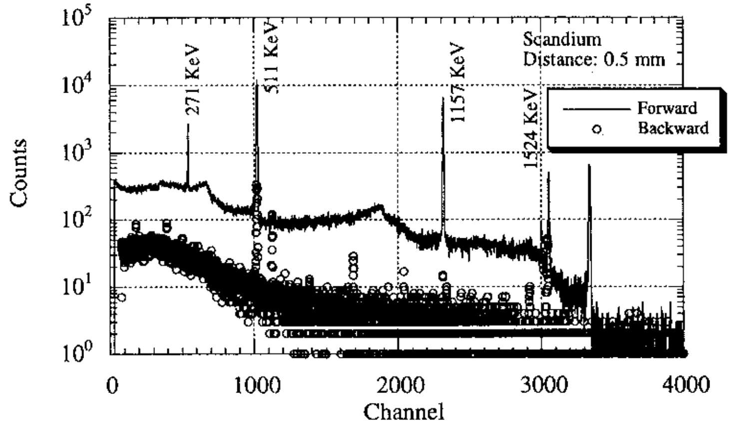

Fig.7 Gamma-ray spectra of radioactivities emitted from scandium target irradiated with 14.9 MeV neutrons.

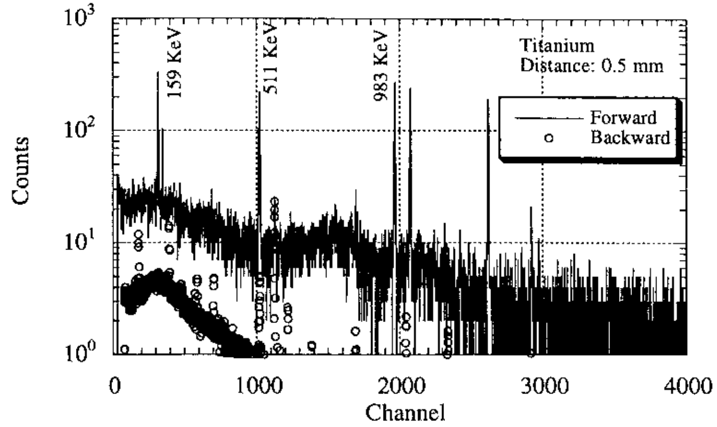

Fig.8 Gamma-ray spectra of radioactivities emitted from titanium target irradiated with 14.9 MeV neutrons.

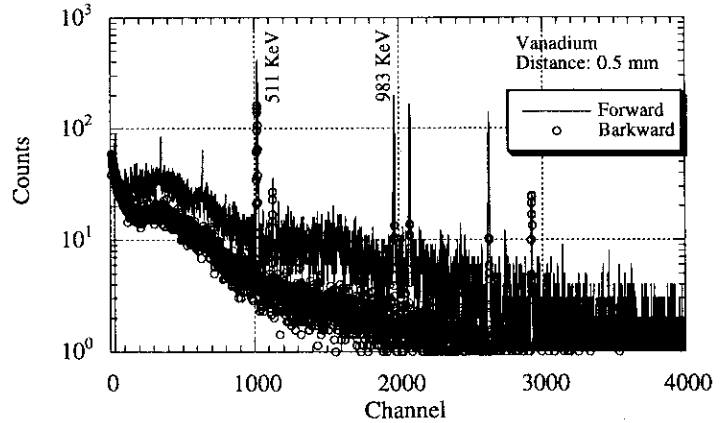

Fig.9 Gamma-ray spectra of radioactivities emitted from vanadium target irradiated with 14.9 MeV neutrons.

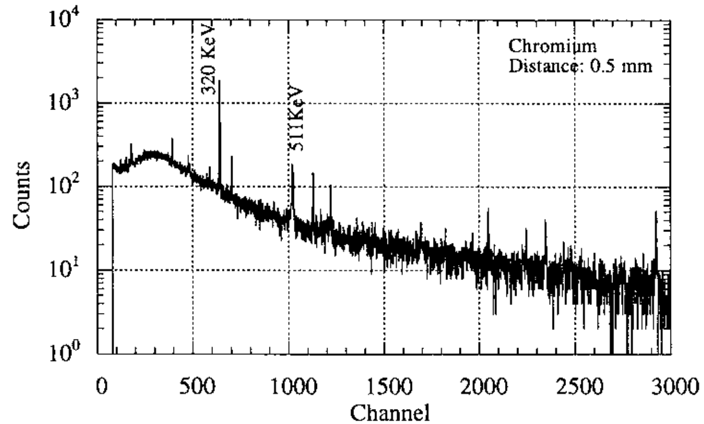

Fig.10 Gamma-ray spectrum of radioactivities emitted from chromium target irradiated with 14.9 MeV neutrons.

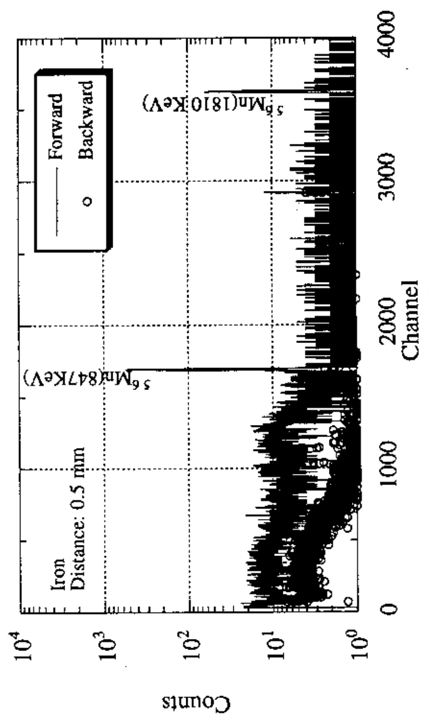

Fig.11 Gamma-ray spectra of radioactivities emitted from iron target irradiated with 14.9 MeV neutrons.

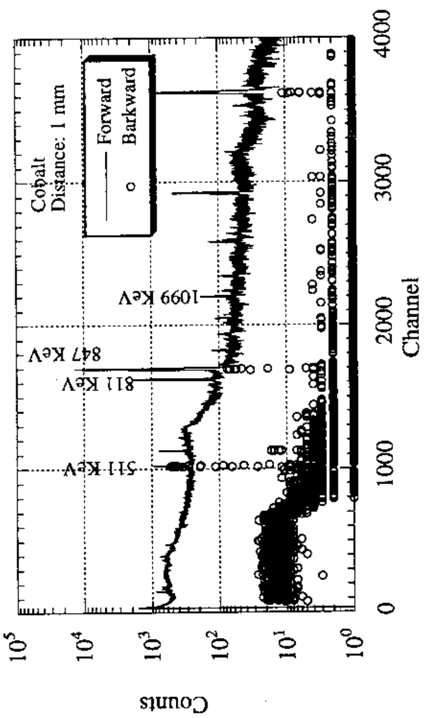

Fig.12 Gamma-ray spectra of radioactivities emitted from cobalt target irradiated with 14.9 MeV neutrons.

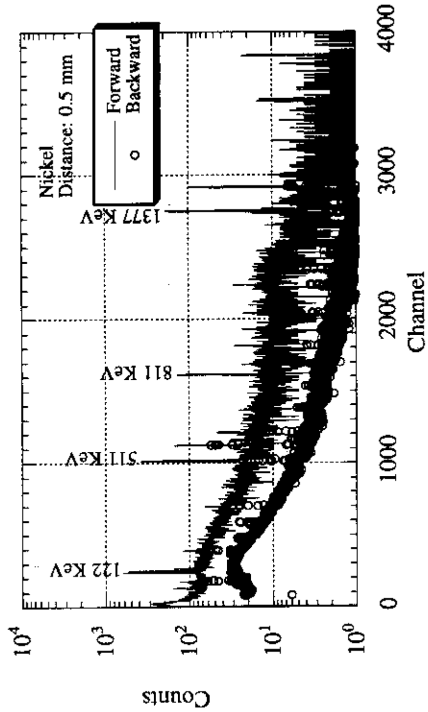

Fig.13 Gamma-ray spectra of radioactivities emitted from nickel target irradiated with 14.9 MeV neutrons.

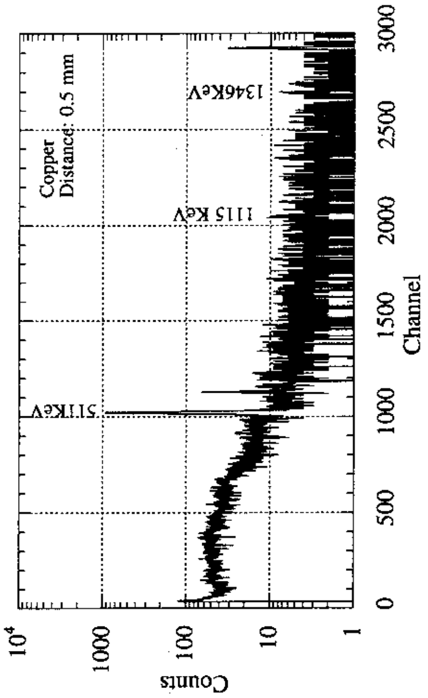

Fig.14 Gamma-ray spectrum of radioactivities emitted from copper target irradiated with 14.9 MeV neutrons.

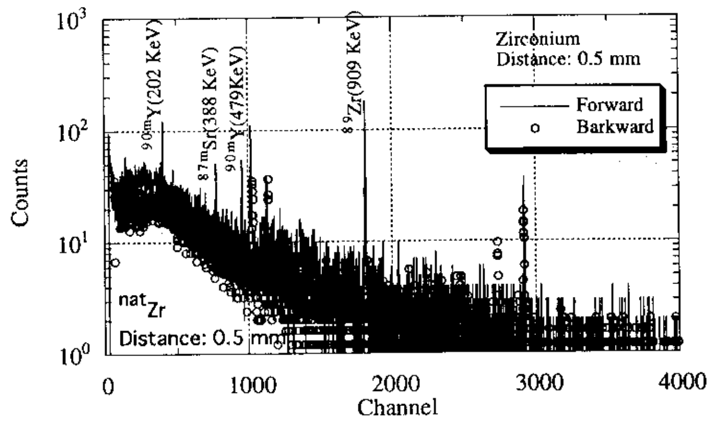

Fig.15 Gamma-ray spectra of radioactivities emitted from zirconium target irradiated with 14.9 MeV neutrons.

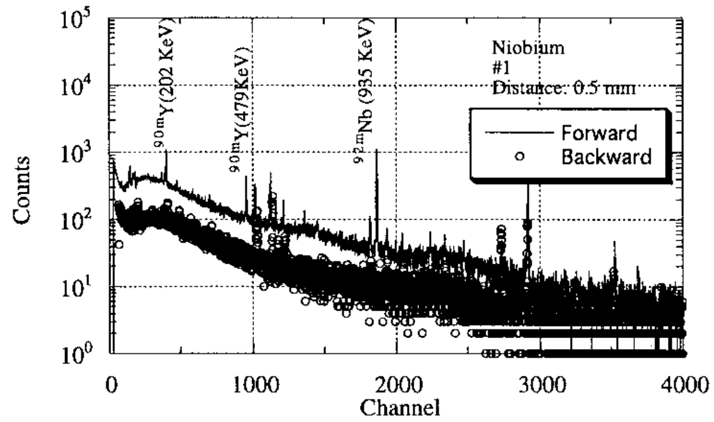

Fig.16 Gamma-ray spectra of radioactivities emitted from the first niobium target irradiated with 14.9 MeV neutrons.

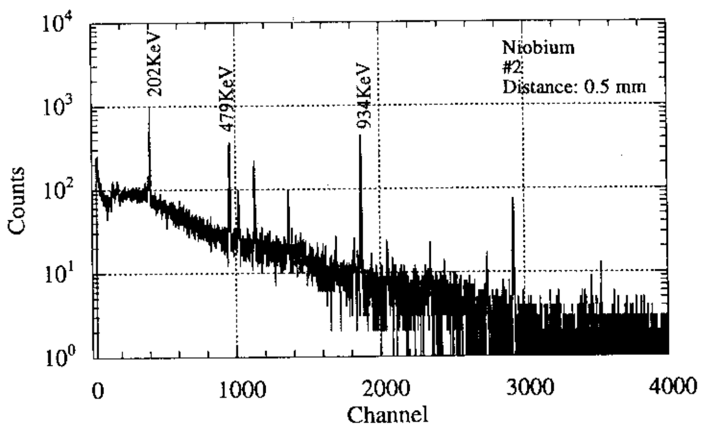

Fig.17 Gamma-ray spectrum of radioactivities emitted from the second niobium target irradiated with 14.9 MeV neutrons.

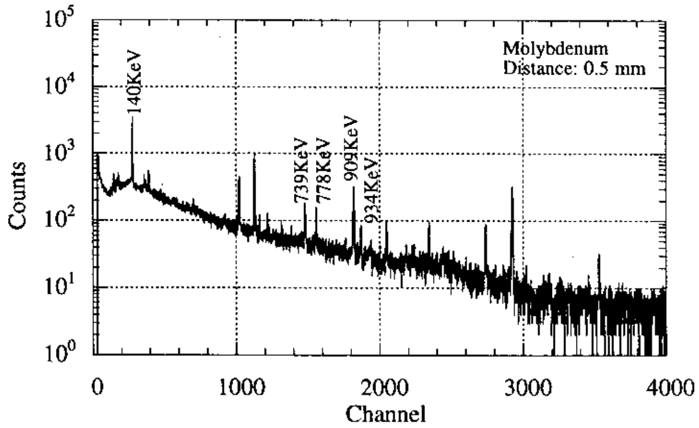

Fig.18 Gamma-ray spectrum of radioactivities emitted from molybdenum target irradiated with 14.9 MeV neutrons.

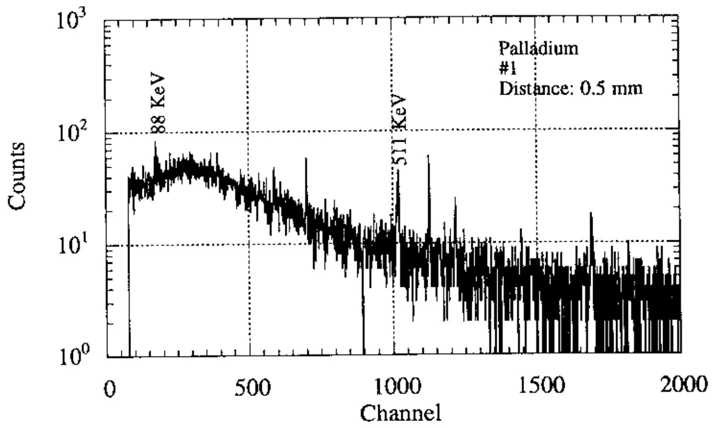

Fig.19 Gamma-ray spectrum of radioactivities emitted from the first palladium target irradiated with 14.9 MeV neutrons.

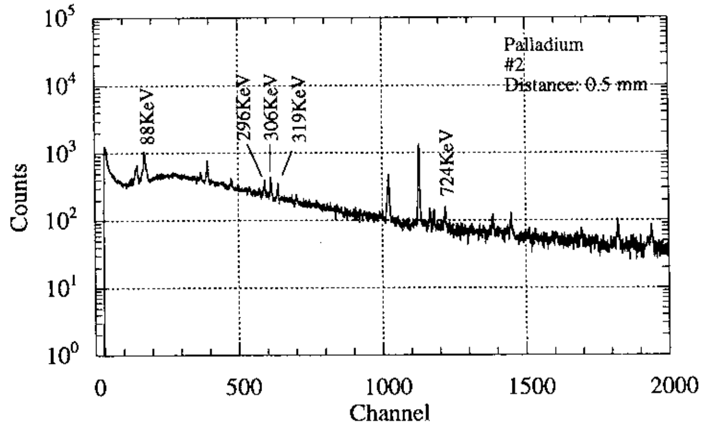

Fig.20 Gamma-ray spectrum of radioactivities emitted from the second palladium target irradiated with 14.9 MeV neutrons.

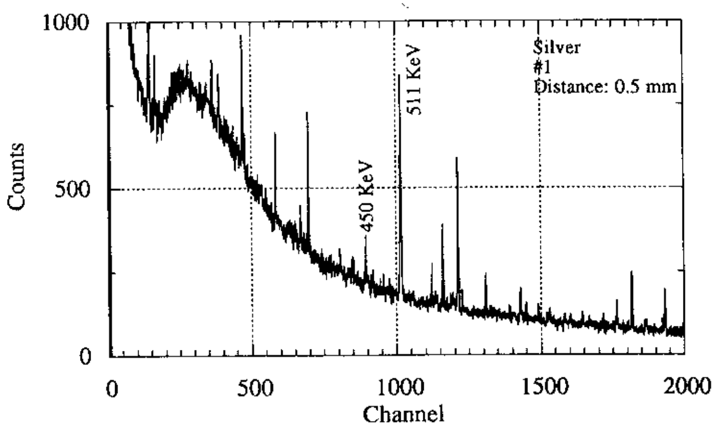

Fig.21 Gamma-ray spectrum of radioactivities emitted from the first silver target irradiated with 14.9 MeV neutrons.

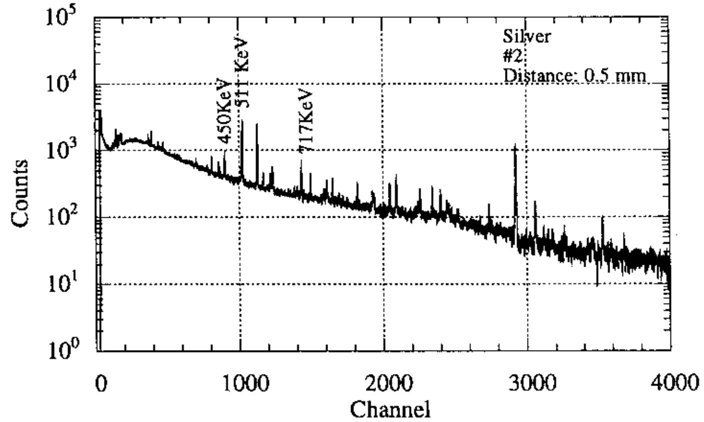

Fig.22 Gamma-ray spectrum of radioactivities emitted from the second silver target irradiated with 14.9 MeV neutrons.

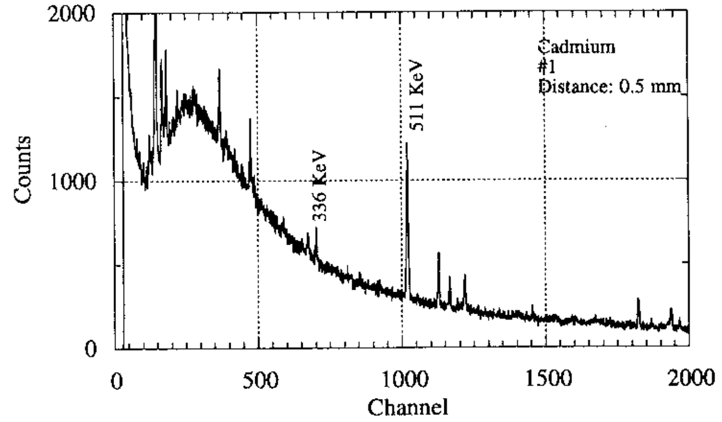

Fig.23 Gamma-ray spectrum of radioactivities emitted from the first cadmium target irradiated with 14.9 MeV neutrons.

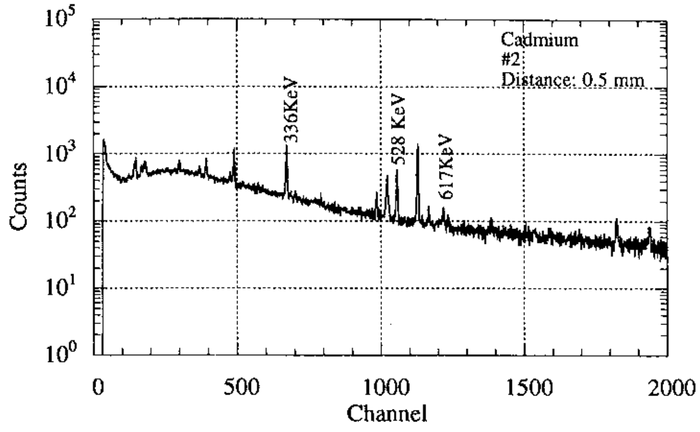

Fig.24 Gamma-ray spectrum of radioactivities emitted from the second cadmium target irradiated with 14.9 MeV neutrons.

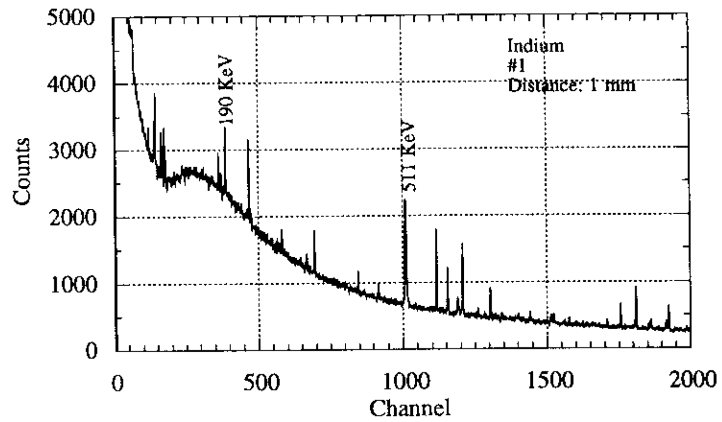

Fig.25 Gamma-ray spectrum of radioactivities emitted from the first indium target irradiated with 14.9 MeV neutrons.

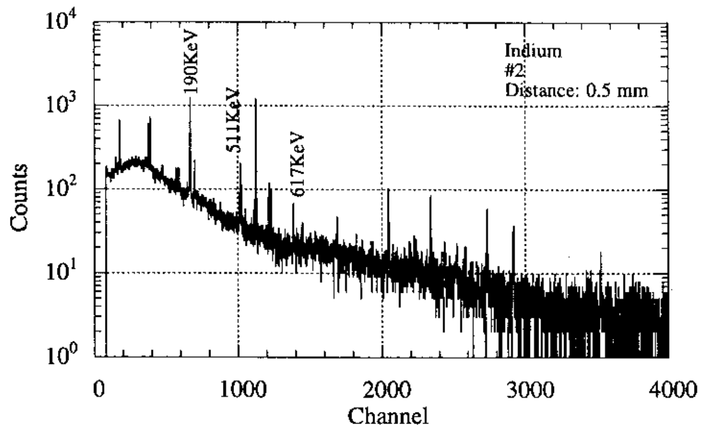

Fig.26 Gamma-ray spectrum of radioactivities emitted from the second indium target irradiated with 14.9 MeV neutrons.

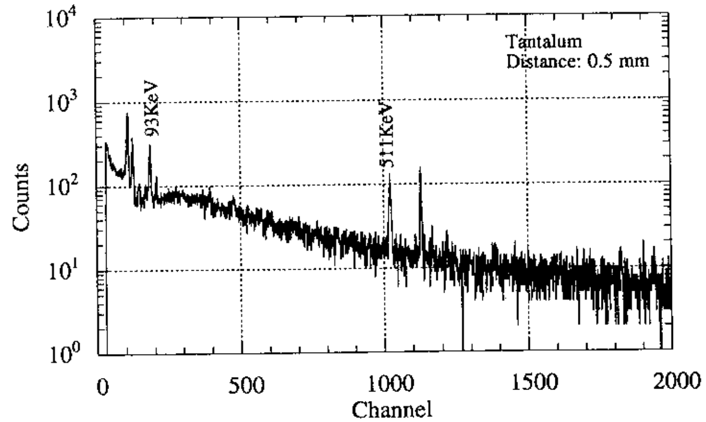

Fig.27 Gamma-ray spectrum of radioactivities emitted from tantalum target irradiated with 14.9 MeV neutrons.

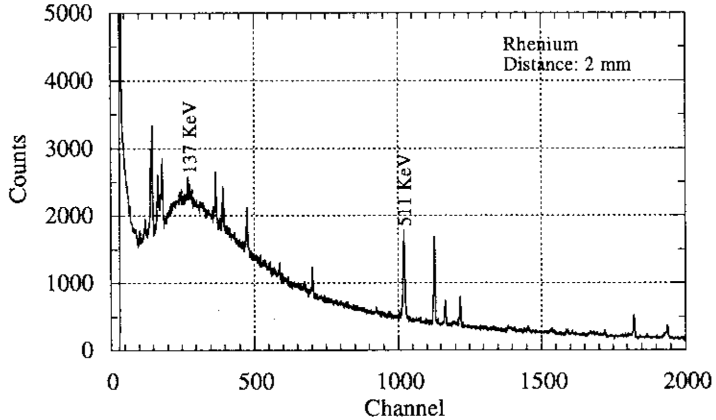

Fig.28 Gamma-ray spectrum of radioactivities emitted from rhenium target irradiated with 14.9 MeV neutrons.

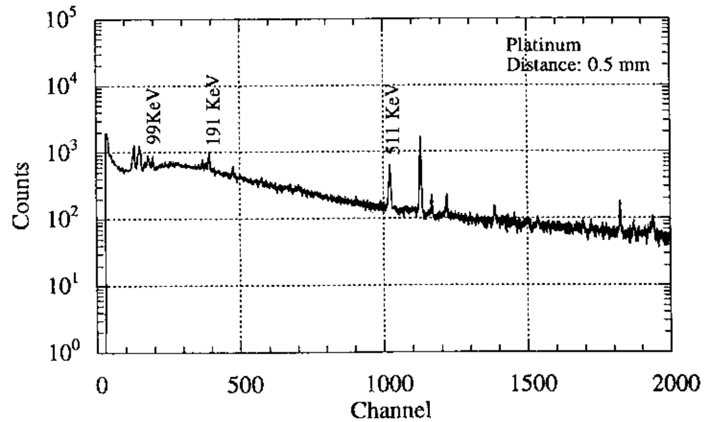

Fig.29 Gamma-ray spectrum of radioactivities emitted from platinum target irradiated with 14.9 MeV neutrons.

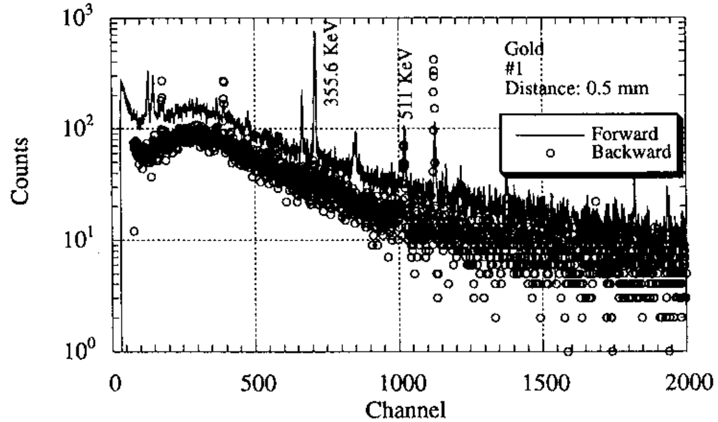

Fig.30 Gamma-ray spectra of radioactivities emitted from the first gold target irradiated with 14.9 MeV neutrons.

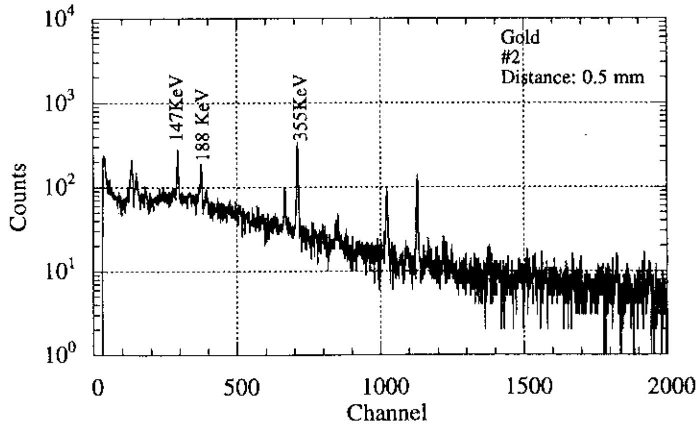

Fig.31 Gamma-ray spectrum of radioactivities emitted from the second gold target irradiated with 14.9 MeV neutrons.

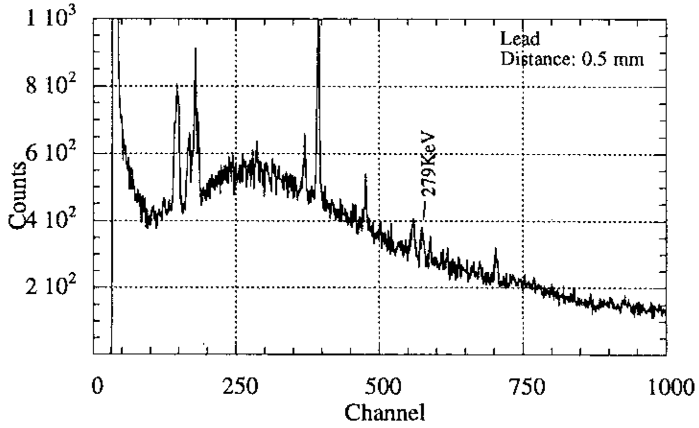

Fig.32 Gamma-ray spectrum of radioactivities emitted from lead target irradiated with 14.9 MeV neutrons.

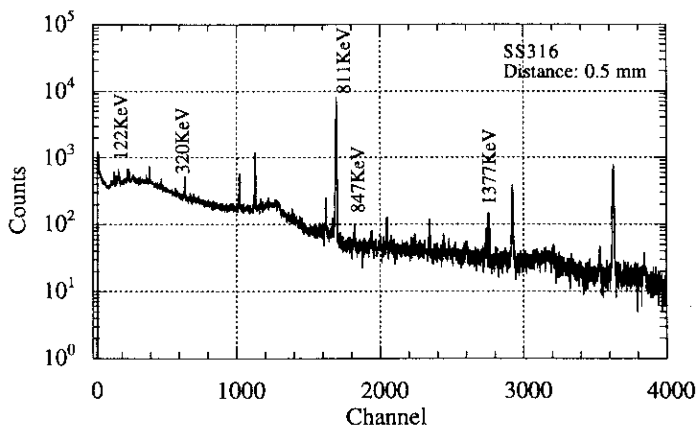

Fig.33 Gamma-ray spectrum of radioactivities emitted from stainless steel 316 target irradiated with 14.9 MeV neutrons.

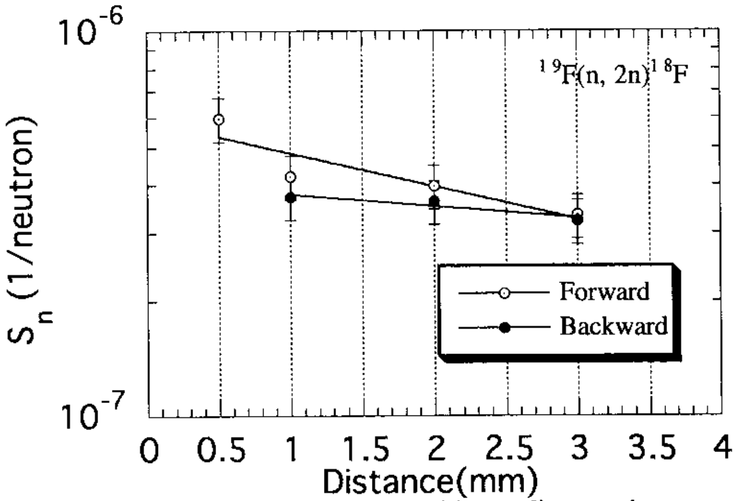

Fig.34 Dependency of activity intensities on distances between target and collectors for fluorine.

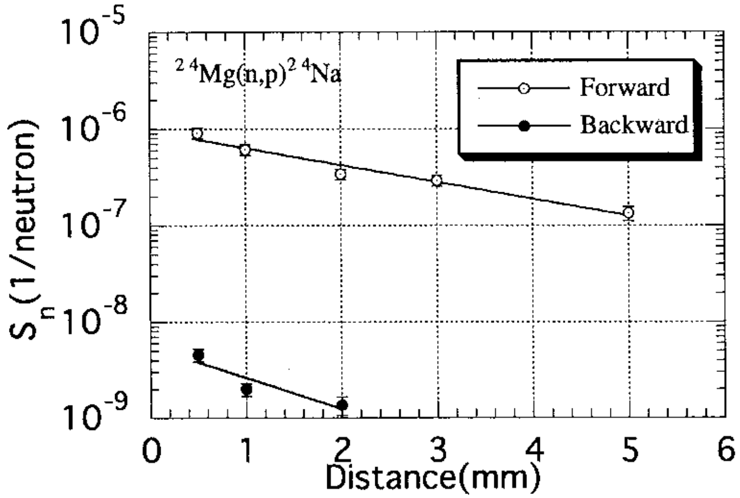

Fig.35 Dependency of activity intensities on distances between target and colleators for magnesium.

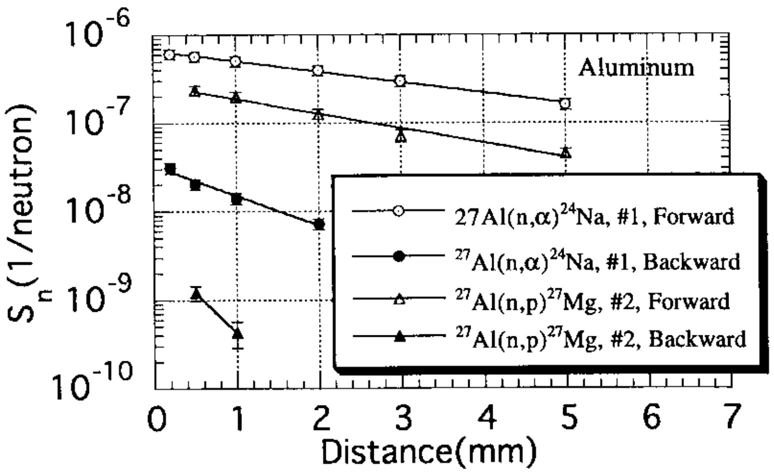

Fig.36 Dependency of the sputtering yield on distances between target and collectors for aluminum.

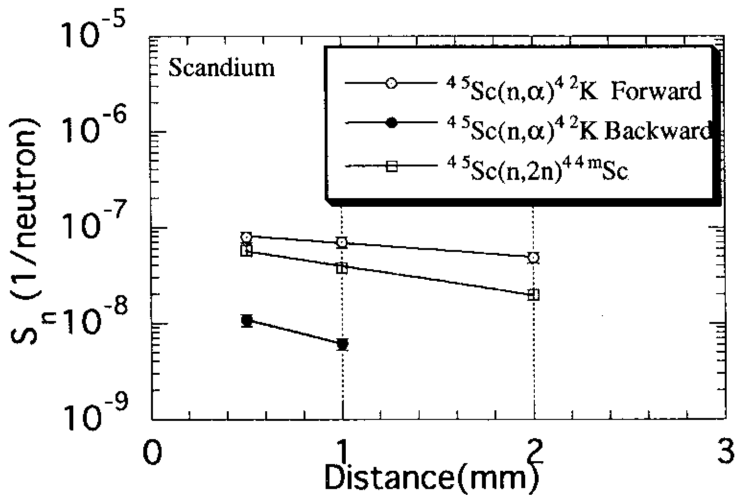

Fig.37 Dependency of activity intensities on distances between target and collectors for scandium.

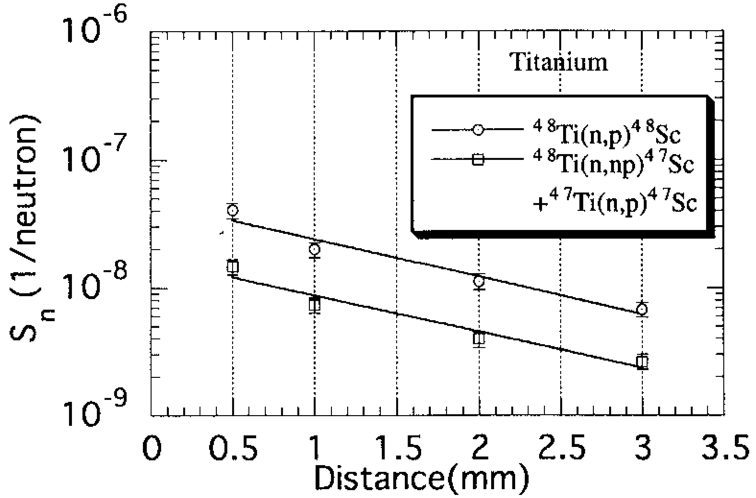

Fig.38 Dependency of activity intensities on distances between target and collectors for titanium.

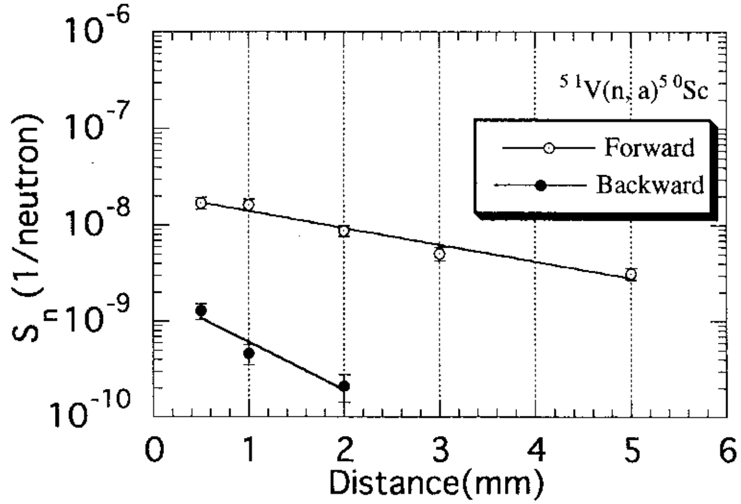

Fig.39 Dependency of activity intensities on distances between target and collectors for vanadium.

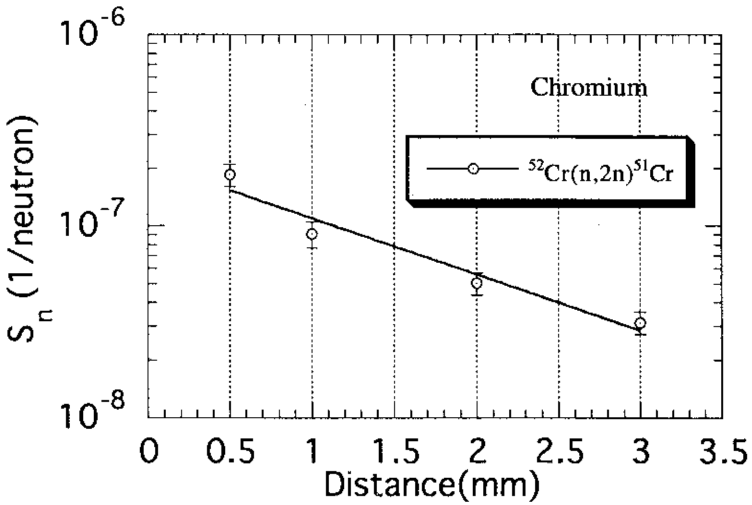

Fig.40 Dependency of activity intensities on distances between target and collectors for chromium.

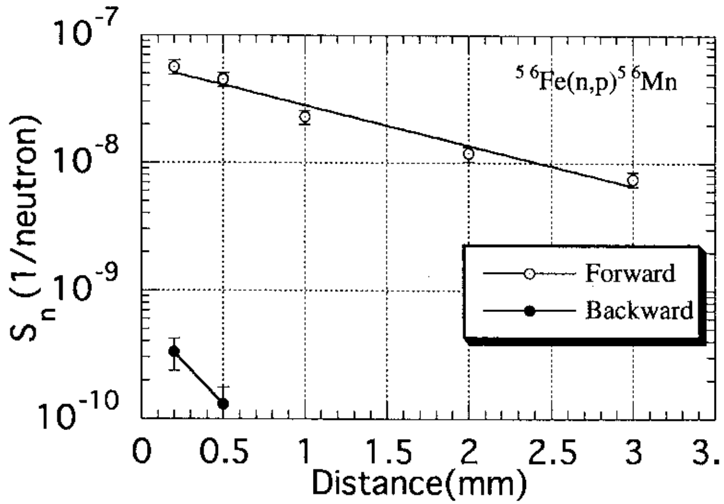

Fig.41 Dependency of activity intensities on distances between target and collectors for iron.

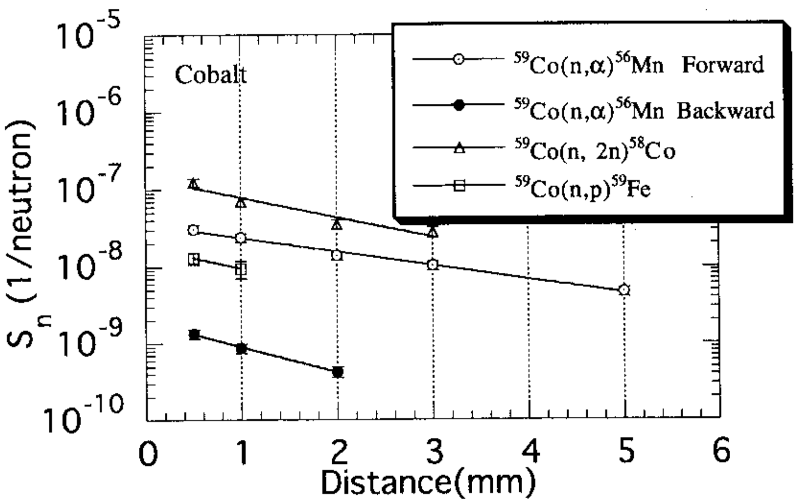

Fig.42 Dependency of activity intensities on distances between target and collectors for cobalt.

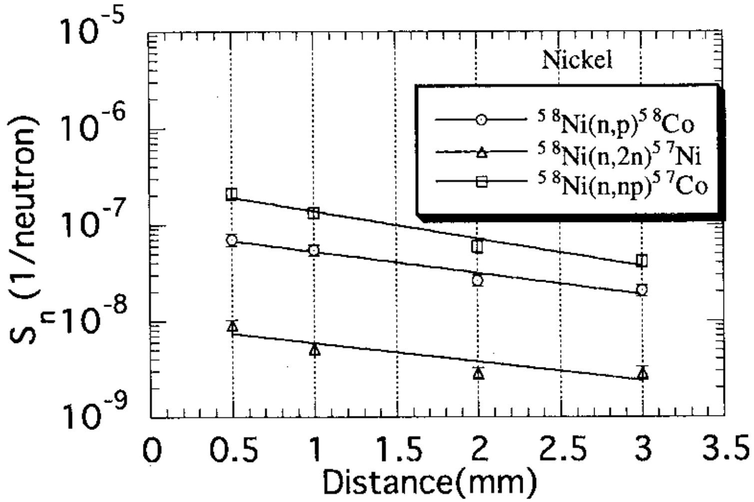

Fig.43 Dependency of activity intensities on distances between target and collectors for nickel.

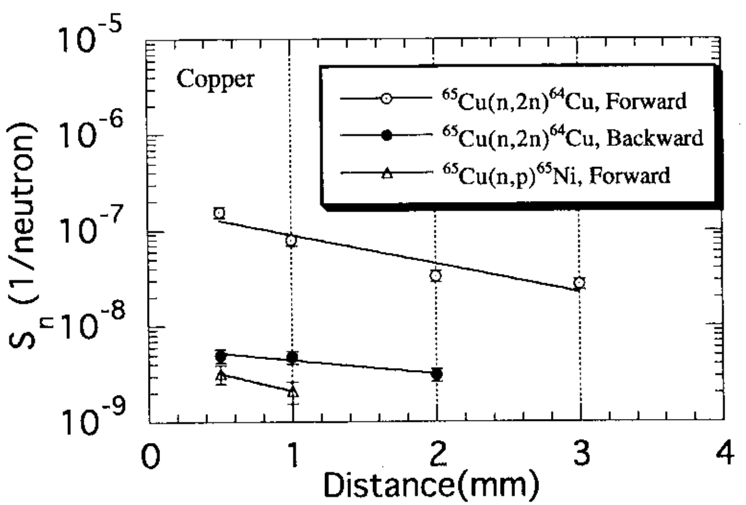

Fig.44 Dependency of activity intensities on distances between target and collectors for copper.

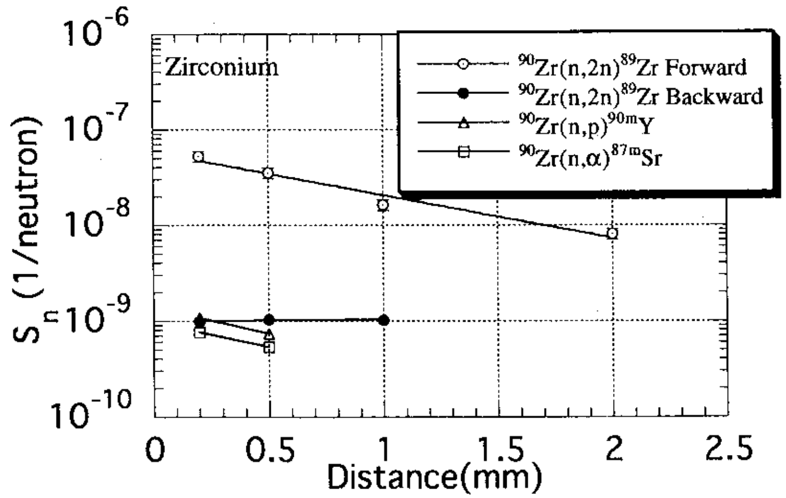

Fig.45 Dependency of activity intensities on distances between target and collectors for zirconium.

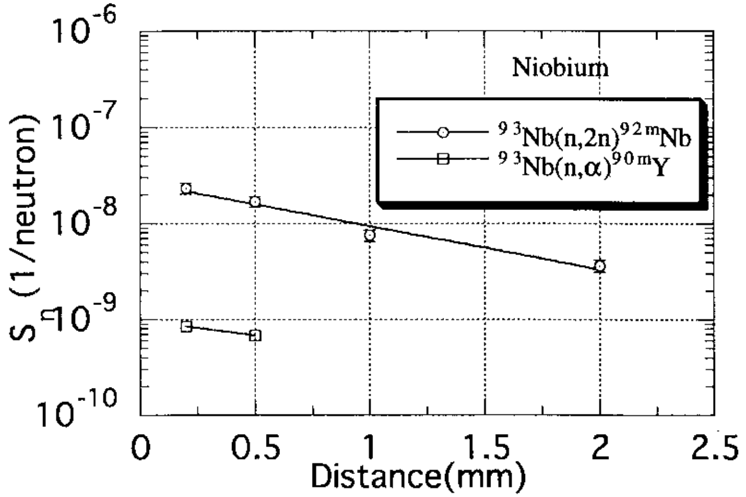

Fig.46 Dependency of activity intensities on distances between target and collectors for niobium.

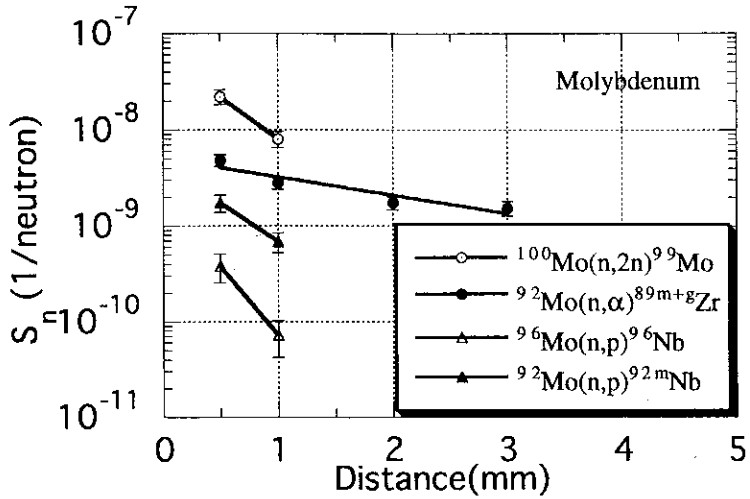

Fig.47 Dependency of activity intensities on distances between target and collectors for molybdenum.

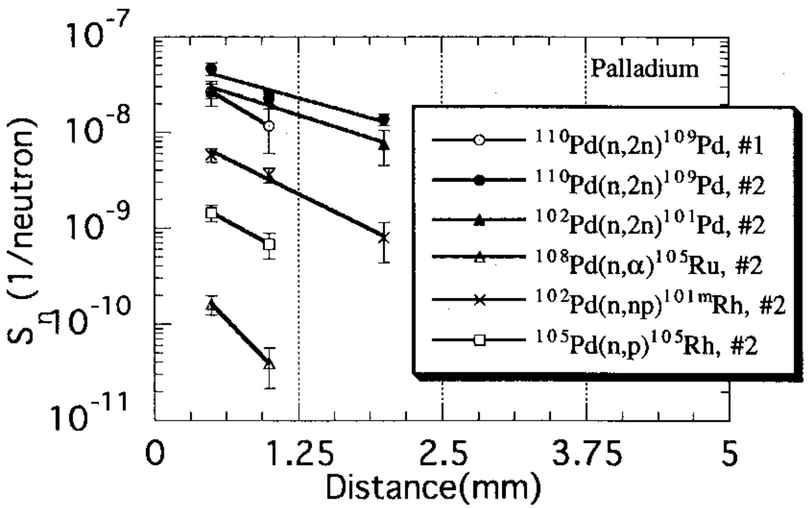

Fig.48 Dependency of activity intensities on distances between target and collectors for palladium.

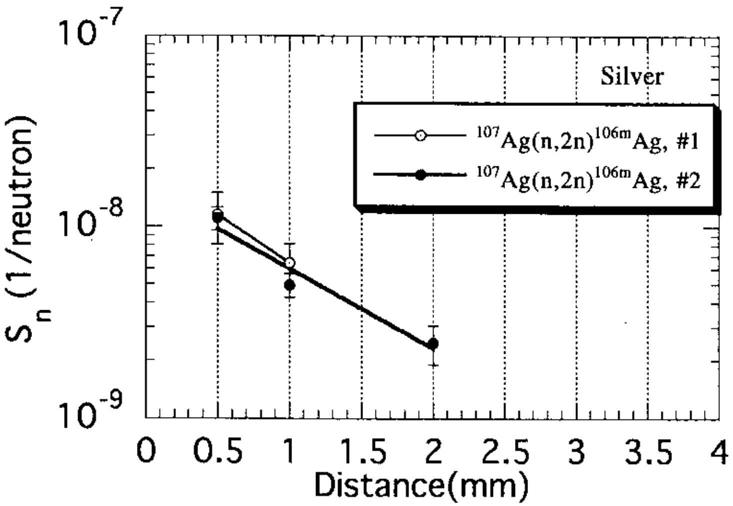

Fig.49 Dependency of activity intensities on distances between target and collectors for silver.

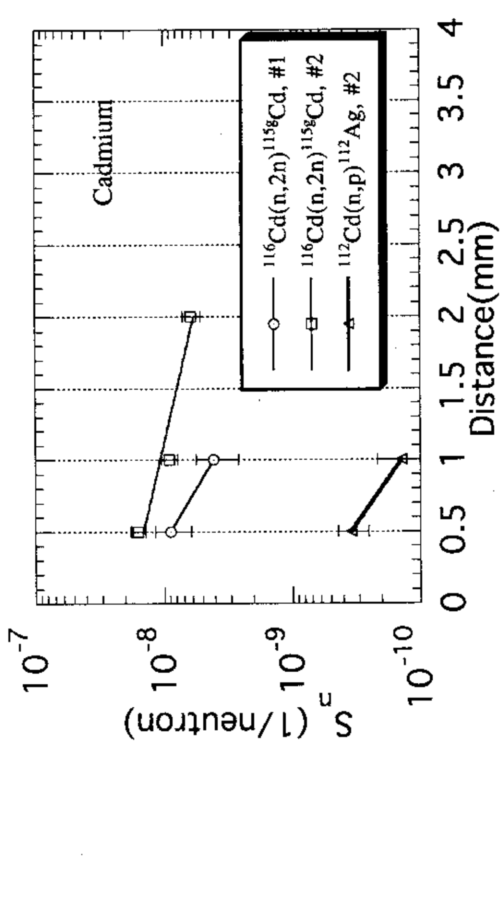

Fig.50 Dependency of activity intensities on distances between target and collectors for cadmium.

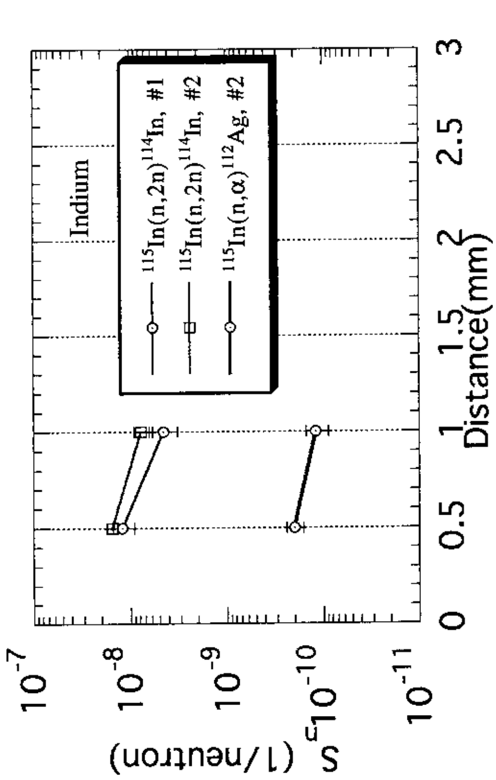

Fig.51 Dependency of activity intensities on distances between target and collectors for indium.

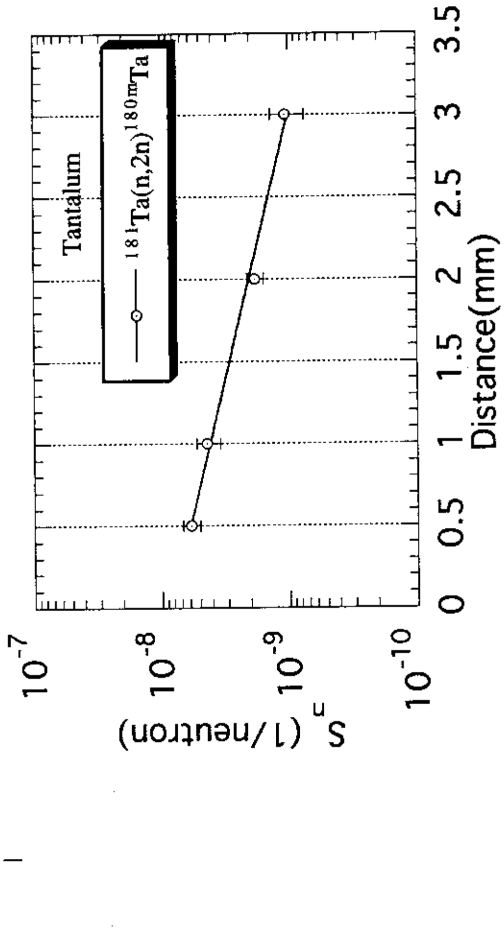

Fig.52 Dependency of activity intensities on distances between target and collectors for tantalum.

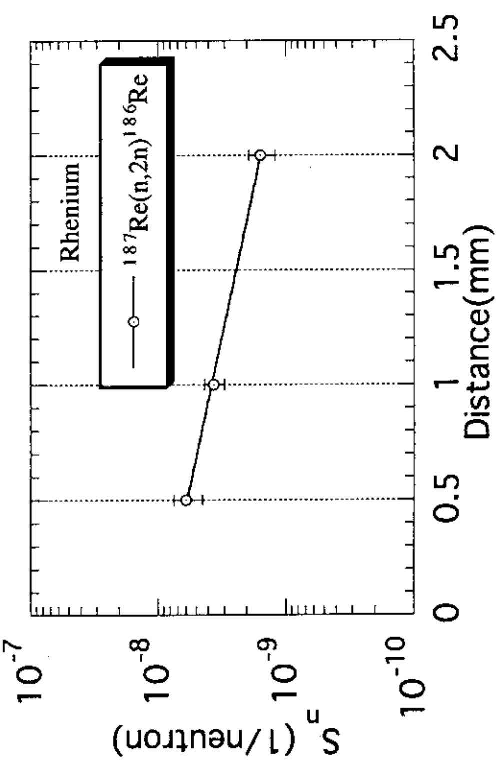

Fig.53 Dependency of activity intensities on distances between target and collectors for rhenium.

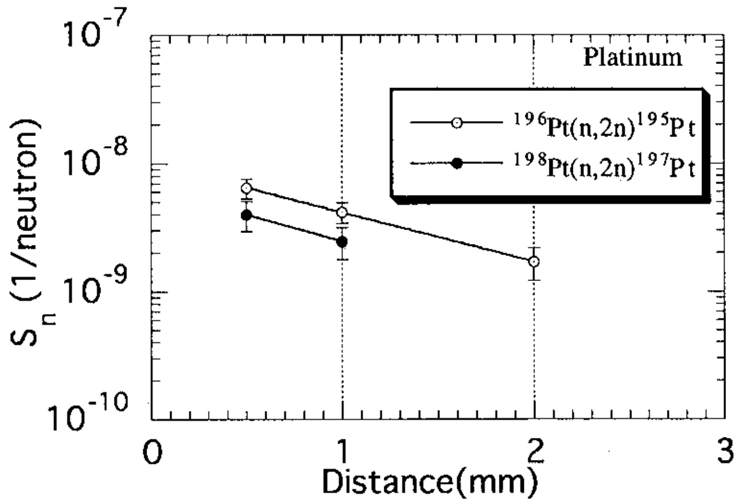

Fig.54 Dependency of activity intensities on distances between target and collectors for platinum.

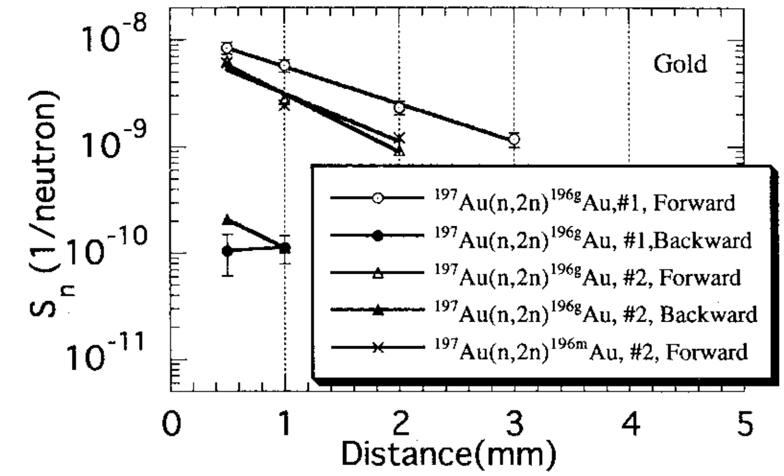

Fig.55 Dependency of activity intensities on distances between target and collectors for gold.

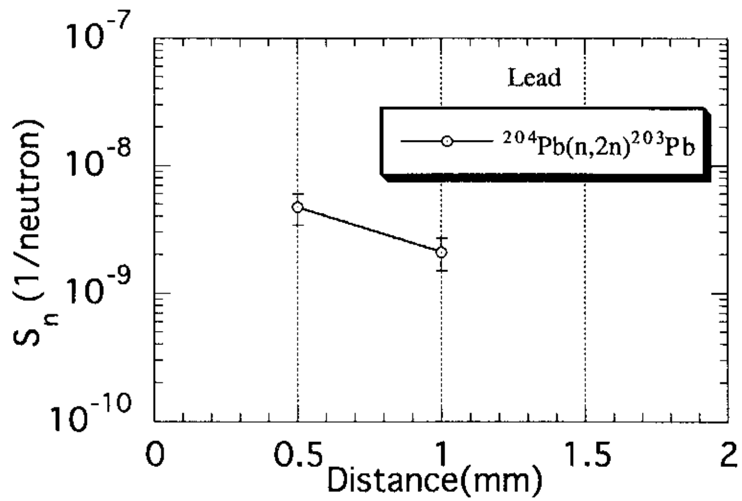

Fig.56 Dependency of activity intensities on distances between target and collectors for lead.

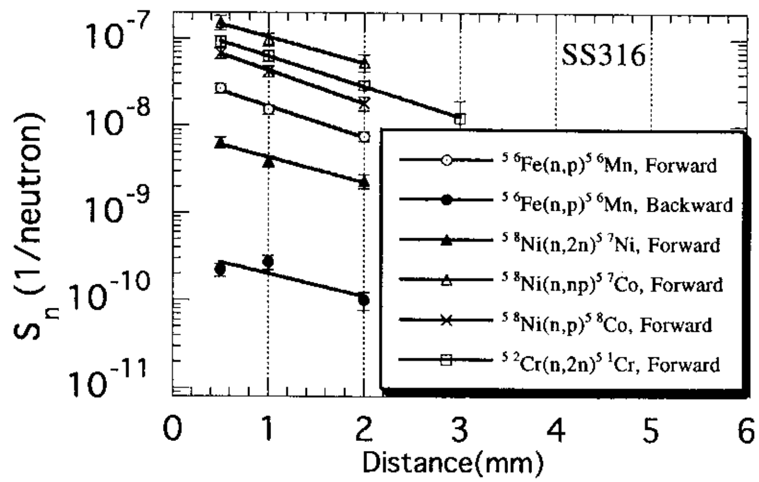

Fig.57 Dependency of activity intensities on distances between target and collectors for stainless steel 316.

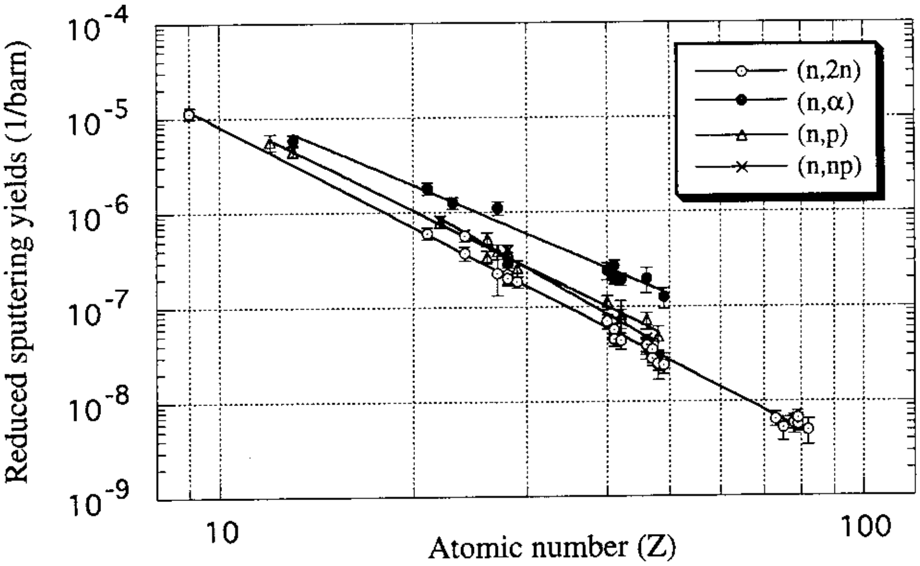

Fig.58 The systematic trends of reduced sputtering yields as a function of atomic numbers (Z) of target materials for (n,2n), (n,α) , (n,p) and (n,np) reactions.

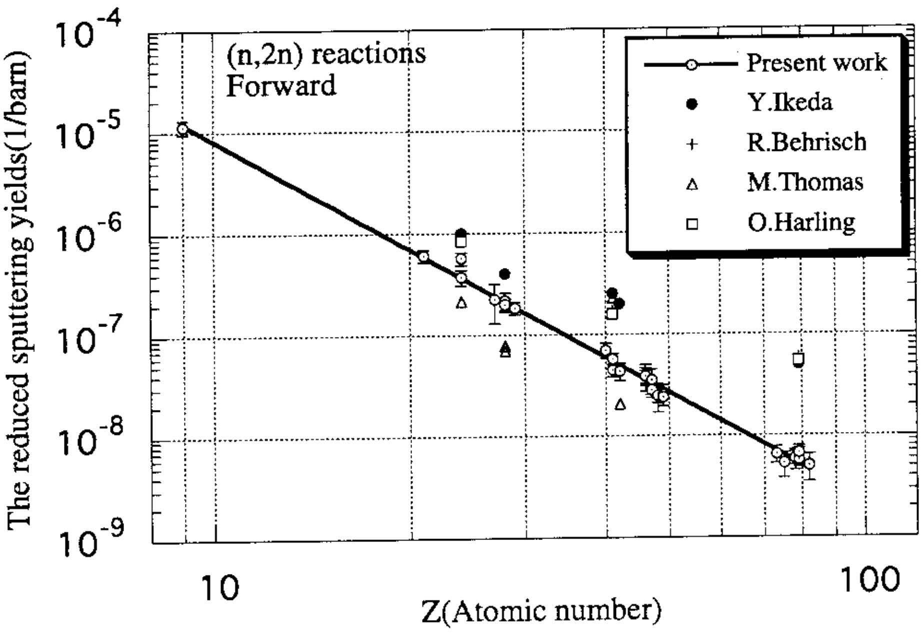

Fig.59 Comparison of present results with other results for (n, 2n) reaction.

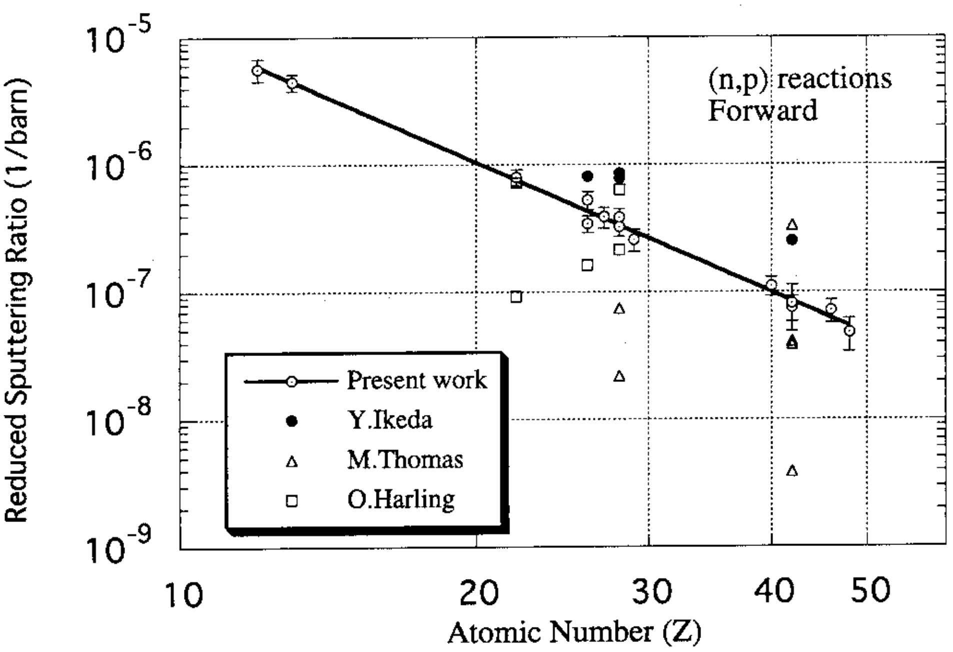

Fig.60 Comparison of present results with other results for (n,p) reaction.

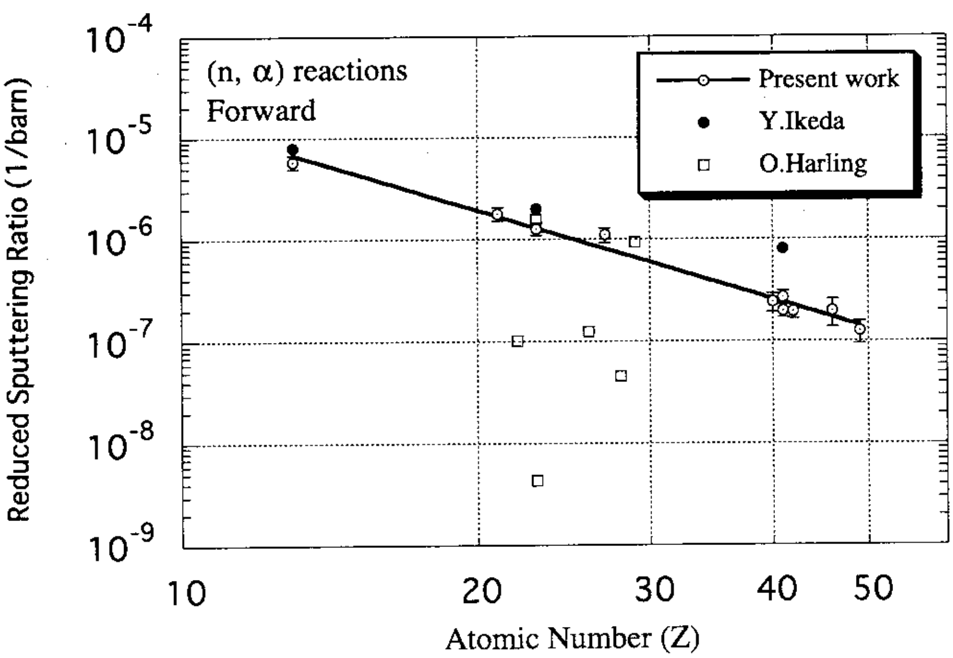

Fig.61 Comparison of present results with other results for (n, α) reaction.

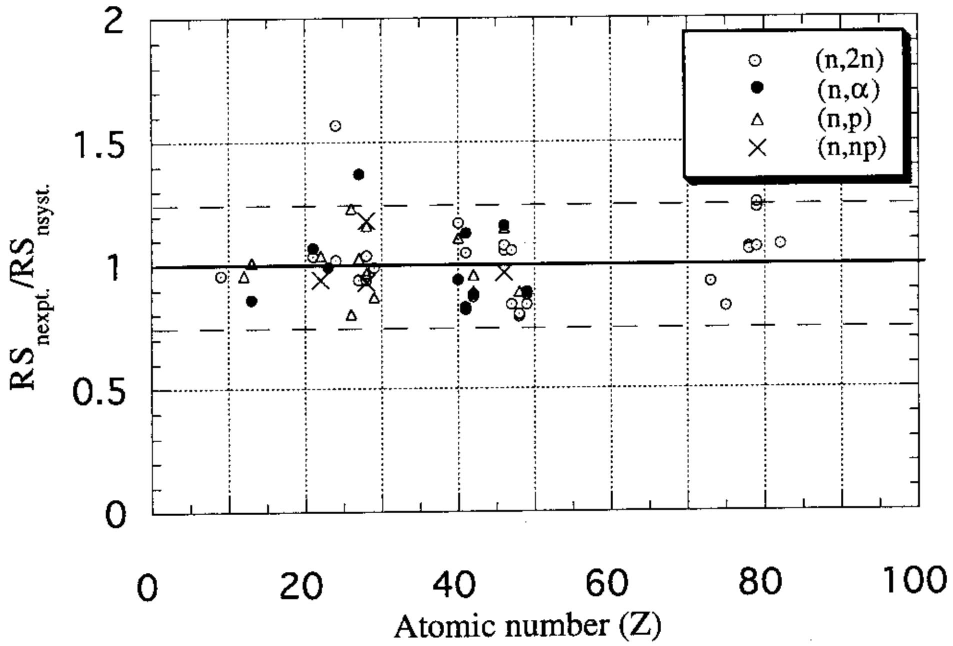

Fig.62 The ratios between the experimental RS_n and the systematical RS_n are plotted with respect to atomic number (Z).

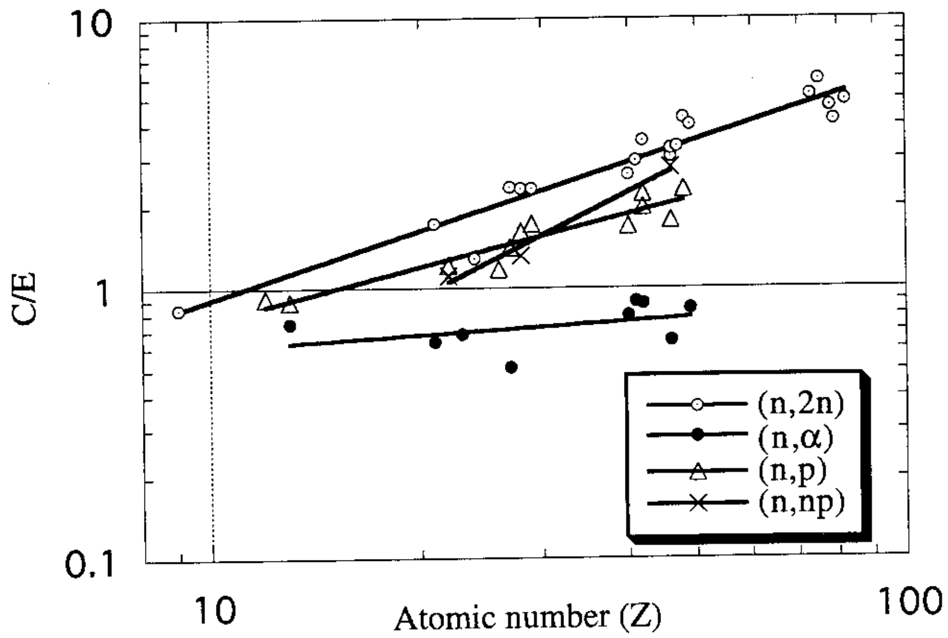

Fig.63 The ratios C/E was plotted according to the type of reactions.